CRYSTALLINITY IN ATACTIC POLYVINYL CHLORIDE

proefschrift

ter verkrijging van de graad van doctor in de technische wetenschappen aan de Technische Hogeschool Delft, op gezag van de rector magnificus ir. H. R. van Nauta Lemke, hoogleraar in de afdeling der elektrotechniek, voor een commissie uit de senaat te verdedigen op woensdag 5 januari 1972 te 14.00 uur door

Johannes Anthonij Juijn

scheikundig ingenieur
geboren te Vlaardingen

1972
Drukkerij J.H. Pasmans – 's-Gravenhage

Dit proefschrift is goedgekeurd door de promotor

Prof.ir. W.A. de Jong

en is tot stand gekomen onder direct toezicht van

Dr. J.H. Gisolf

lector aan de Technische Hogeschool Delft.

Helma, Koos,

Beert, Bert, Dick, Ed, Eric,
Evert, Fred, Herman, Henk, Jaap,
Jacob, Jan, Jan, Joep, Kees,
Leen, Louis, Miel, Pieter Jan,
Rien, Ries, Wim, Wijnand,

en vooral

Aad,

hartelijk bedankt voor jullie
medewerking.

CONTENTS

CHAPTER 1

INTRODUCTION, AIM OF THIS STUDY

Crystallinity in a material can occur when a regular spatial arrangement of the molecules of that material is possible.For this reason most low molecular compounds are able to form a crystalline phase. For high molecular compounds, however, particularly polymers, the formation of such a regular spatial arrangement is much more difficult.

The first problem in polymer crystallization is caused by the chain form of the molecules. It is rather usual that the length of polymer molecules is 1000 times their thickness. The crystallization of these long chain molecules causes problems very similar to those of a woman who is trying to knit with a knotted ball of wool: after a short time she is left with an inextricable clew, and she is ready to cut the thread in anger. By comparison, this is the moment that the polymer has reached its maximum amount of crystallinity. The knitting which was finished represents the crystalline phase and the remainder of the disordered ball of wool the amorphous phase.

The second factor is the ease with which crystallization occurs which depends on the chemical structure of the polymer and, hence, on its molecular conformation. Polyethylene, for example, crystallizes very readily; its simple chemical structure enables the chains to assume the highly regular extended zig-zag conformation. However, many other polymers crystallize with difficulty or not at all. There are two main reasons for the non-crystalline behaviour of these polymers: lack of tacticity and the occurrence of steric hindrance.

The polymer discussed in the present thesis, polyvinyl chloride or PVC, belongs to the second group, *viz.* the polymers that do not form crystals as readily as polyethylene. In PVC the two stereoisomeric forms of the monomer give rise to different conformations of the chain. A part of the chain which is syndiotactic can have a planar zig-zag

conformation. In that case the chlorine atoms are placed alternately at the sides of the plane of the zig-zag chain. This spatial arrangement is energetically favoured over other syndiotactic conformations and at the same time it is a very regular chain structure which can contribute to the formation of crystalline structures. With an isotactic part of the chain, however, the zig-zag chain structure is not possible. Here, the chlorine atoms should all be placed at one side of the chain, but this is impossible because of steric hindrance. Therefore the isotactic chain parts have other conformations which were thought to be hardly or not at all crystallizable.

During the technical polymerization of vinyl chloride at temperatures of 40 - 75°C, syndiotactic propagation is only slightly favoured over isotactic propagation. As a result, a commercial PVC is atactic, which means that about 50% of the monomer sequences in the chain are syndiotactic, the remaining 50% being isotactic. Syndiotactic sequences are randomly distributed along the chain and, therefore, long syndiotactic or isotactic sequences do not occur.

Here we have arrived at the basic question of this thesis. Although commercial PVC is known to be atactic, it is also well established that its crystalline content amounts to about 10%. This relatively "high" crystallinity is not in accord with the "low" tacticity of the material if one assumes that only syndiotactic PVC is crystallizable. It is the aim of this work to explain the occurrence of crystallinity in atactic PVC by studying the tacticity, the chain conformations and the crystalline structures in PVC.

Literature data concerning measurements of the tacticity by means of infrared and nuclear magnetic resonance techniques are reviewed in chapter 2. The influence of the polymerization temperatures on the tacticity is also considered. Then, the attempt is made to calculate and explain the crystallinity of atactic PVC by means of Flory's theory.

Experimental work is presented in the chapters 3 and 4.

The melting of crystallites of PVC was studied by means of Differen-

tial Scanning Calorimetry. Crystallite melting effects were found in atactic commercial PVC as well as in laboratory-prepared syndiotactic PVC. In untreated virgin PVC, melting of crystals was detected at temperatures above 150°C. Annealing of PVC at temperatures above the glass transition temperature was found to produce crystallinity. These effects are described in chapter 3.

The formation of crystalline structures by annealing has an important consequence for the behaviour of plasticized PVC compounds. In chapter 4 the physical aging of plasticized PVC is explained as a crystallization process which causes the stiffness and the density of the material to increase.

The experimental work clearly shows that considerable crystalline effects occur in atactic PVC. This atactic crystallinity cannot be explained by the classical interpretation of Flory's theory, *viz.* that only syndiotactic chain segments crystallize. Therefore, a theoretical study on the chain structure and the crystalline packing of syndiotactic as well as isotactic chain segments was performed.

In chapter 5 the results of studies on the structure of the chain are presented. Conformations of syndiotactic and isotactic sequences are given. A special isotactic chain conformation is introduced which resembles the syndiotactic zig-zag chain structure. The energy of this isotactic straight chain conformation is calculated and compared with the chain energies of the syndiotactic zig-zag chain and the isotactic helix. A literature survey of the infrared studies on chain conformations of PVC is presented and the existence of the isotactic straight chain conformation is discussed in the light of the available information. Literature studies on the crystalline packing, especially by X-ray analysis, are reviewed in chapter 6. The present work shows that atactic chain segments can crystallize in a way which is similar to that described by other authors for the entirely syndiotactic chains. On the basis of this new concept the amount of crystallinity in an atactic PVC is calculated.

Finally, a general interpretation of the crystalline effects in PVC is presented.

CHAPTER 2

TACTICITY AND CRYSTALLINITY OF PVC

2.1. Tacticity

Polyvinyl chloride, $(-CH_2-CHCl-)_n$, can be a stereoregular polymer since there are two different arrangements of the chlorine atom in the CHCl group. The usual way of defining the two stereoregular forms of the polymer chain, syndiotactic and isotactic, has several disadvantages. This definition uses the presentations of zig-zag chains shown in figure 2.1. The carbon atoms lie in the plane of the paper, bonds designated as --- under this plane and those designated as ▬ above it.

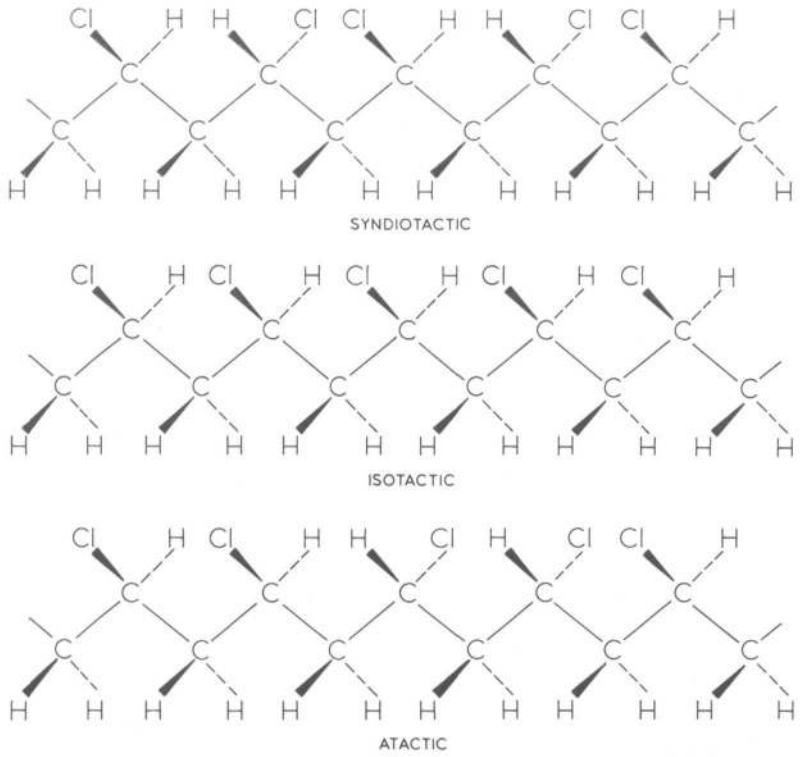

Figure 2.1. Stereoregularity of PVC.
a-syndiotactic; b-isotactic; c-atactic

In the syndiotactic configuration the chlorine atoms are placed in alternating positions around the zig-zag chain backbone. The configuration of figure 2.1b, where the chlorine atoms are all indicated as situated on the same side of the backbone (which is, in fact, impossible because of steric hindrance between contiguous chlorine atoms!) is called isotactic. The atactic configuration is shown in figure 2.1c; this configuration must be regarded as a random distribution of the syndiotactic and isotactic form.

The above presentation suggests that tacticity depends on the spatial arrangement of the carbon backbone. This is not true: the configuration is independent of the conformation.

It is important to use the words configuration and conformation in a proper way. In this thesis the IUPAC rules[1] are obeyed.

Configuration: The configuration of a molecule of defined constitution is the arrangement of its atoms in space without regard to arrangements that differ only as after rotation about one or more single bonds.

Conformation: The conformations of a molecule of defined configuration are the various arrangements of its atoms in space that differ only as after rotation about single bonds.

However, some structures differ in configurational as well as conformational respects. In such cases the word conformation will be used in this thesis to describe the differences.

For a better description of the relation between chain structure and crystallinity a more adequate definition of tacticity is required[2]. To simplify the discussion, the PVC chain is thought of as exclusively consisting of monomer units connected to each other in the manner shown in figure 2.2. This is the "head-to-tail" addition which predominates in PVC; in other words, the presence in the chain of different sequences and end groups is not considered. A discussion on the way of monomer addition during polymerization is given in the first section of chapter 3.

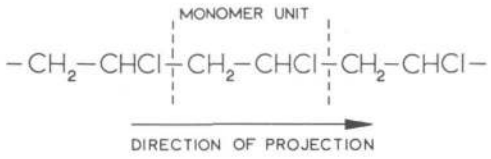

Figure 2.2. Division of the PVC chain into monomer units.

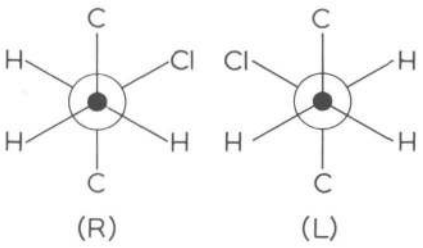

Figure 2.3. Newman projections of the right-handed and left-handed monomer unit.

The monomer units have two stereoisomeric forms that are shown as Newman projections in figure 2.3. The direction of projection indicated in figure 2.2. was chosen; the CH_2 group lies in front of the CHCl group. The methylene carbon atom is designated as ● and the carbon atom of the CHCl group as ◯. It is apparent from figure 2.3. that the relative positions of the hydrogen and the chlorine atom differ in the two cases shown. This is the basis for the two stereoisomeric forms of the monomer.

A monomer in the chain is called *right-handed* (R) if the chlorine atom is situated on the right side of the hydrogen atom (clockwise, angle of rotation: 120°). A monomer unit is called *left-handed* (L) when the relative position of the chlorine atom is described by a counter-clockwise rotation of 120°. A combination of two successive monomer units in the chain (L)(R) or (R)(L) is called *syndiotactic*, the combinations (L)(L) and (R)(R) are called *isotactic*. The words syndiotactic and isotactic are often used for chains or chain segments.

For instance, a chain with monomer units --(R)(L)(R)(L)(R)(L)-- is called syndiotactic since all the sequences are syndiotactic. The same applies to an isotactic chain consisting of monomer units --(R)(R)(R)(R)(R)-- or --(L)(L)(L)(L)(L)--. Atactic chains have no configurational order. Here a random distribution of isotactic and syndiotactic monomer sequences exists. The above definition shows that tacticity is independent of the conformation of the carbon backbone.

It is now possible to define the syndiotacticity or, briefly, tacticity, α, of the material as the fraction of syndiotactic sequences in the chain. When the tacticity is about 0.5 the polymer is called atactic; commercial grades PVC are atactic. Values of α below 0.5 do not occur: there is no known polymerization technique that yields isotactic PVC. For an entirely syndiotactic material the tacticity is 1.0.

The tacticity can be measured by means of nuclear magnetic resonance and infrared spectroscopy. The following sections present literature data on these measurements.

2.2. NMR measurements of the tacticity

Tacticity measurements of PVC by nuclear magnetic resonance (NMR) can be performed on solid polymer samples and polymer solutions. The spectra obtained with solid samples are of the 'broad-band' or 'wide-line' type. Dissolved samples give 'high-resolution' spectra. For the measurements of the tacticity of PVC only the high resolution technique is suitable[3-8].

The spectrum of PVC consists of two main parts: a multiplet centered at about 5.5 τ, corresponding to the methine protons or α protons and a group of peaks around 7.9 τ for the methylene or β protons. An example of such a spectrum was taken from Bovey *et al.*[5] and is shown in figure 2.4.

With double resonance techniques the α part of the spectrum consists of three peaks. In undecoupled spectra three overlapping quintuplets give rise to a complex α band. The usual interpretation of the α proton resonance is in terms of triads of monomer units, *viz.* syndiotactic,

isotactic and heterotactic triads; the latter consist of one syndiotactic and one isotactic sequence. An interpretation using pentads of monomer units was advanced recently by Cavalli *et al.*[9].

The CH_2-β band in the decoupled spectrum shows two peaks. Owing to coupling with vicinal α protons, the normal undecoupled spectrum consists of two overlapping triplets. An interpretation in terms of syndiotactic and isotactic diads of monomer units was given by Johnson[10]. The fine structure of the β band was interpreted by Yoshino[11] based on tetrads of monomer units.

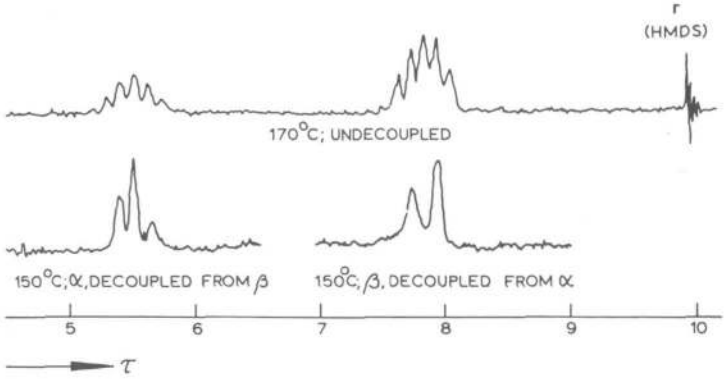

Figure 2.4. NMR spectrum of PVC (According to Bovey *et al.*[5]).

On the basis of the interpretation of the spectrum, *viz.* that certain peaks are ascribed to syndiotactic or isotactic sequences, it is possible to determine the tacticity of PVC from the NMR spectrum. Several authors have estimated the tacticity of PVC as a function of polymerization temperature, using the α part as well as the β region of the spectrum. Their results are collected in table 2.1. and plotted in figure 2.5. For purpose of comparison, curves calculated according to a method outlined in section 4 of this chapter have been added to the experimental points (see also figure 2.7.). The data clearly show that determination from the NMR spectrum yields very inaccurate results.

Table 2.1. Tacticity of PVC as a function of polymerization temperature as determined by NMR

Polymerization temperature, °C	tacticity α calculated from		Reference
	α proton spectrum	β proton spectrum	
100		0.54	Bovey *et al.*[12]
50		0.55	
0		0.57	
- 78		0.63	
40	0.57		Cavalli *et al.*[9]
0	0.61		
- 40	0.65		
52.5	0.55	0.54	Bargon *et al.*[13]
10	0.57	0.58	
0	0.53	0.57	
- 15	0.54	0.55	
- 25	0.56	0.59	
- 30	0.61	0.61	
50		0.61	Enomoto *et al.*[14]
30		0.64	
- 30		0.68	
55		0.60	Satoh[15]
- 30		0.68	
50	0.50	0.55	Tincher[16]
- 20	0.54	0.65	
- 50	0.56	0.68	
- 70	0.60	0.61	
120		0.51	Talamini *et al.*[17]
80		0.53	
60		0.51	
5		0.56	
- 20		0.59	
- 50		0.63	
- 78		0.67	
30		0.51	Germar *et al.*[18]
0		0.59	
- 25		0.54	
- 35		0.73	
- 70		0.80	

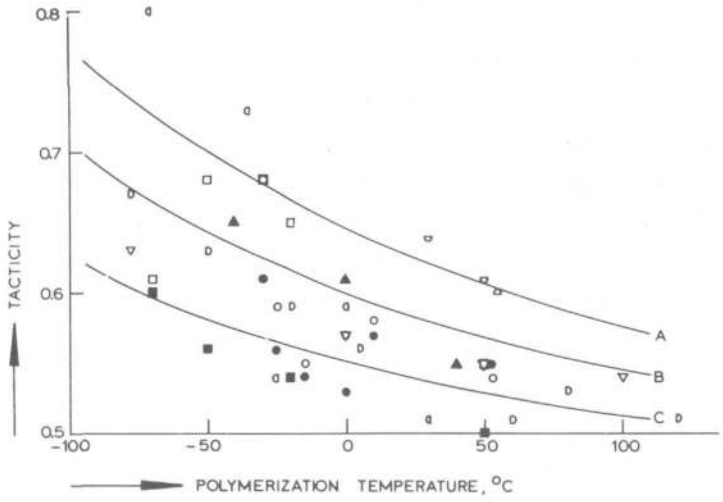

Figure 2.5. Tacticity of PVC as a function of polymerization temperature as measured by NMR.
Black points: estimated from the β part of the NMR spectrum
Open points : estimated from the α part of the NMR spectrum
▽ Bovey *et al.*[12)]
▲ Cavalli *et al.*[9)]
○ and ● Bargon *et al.*[13)]
⌓ Enomoto *et al.*[14)]
⌓ Satoh[15)]
□ and ■ Tincher[16)]
D Talamini *et al.*[17)]
D Germar *et al.*[18)]

2.3. IR measurements of the tacticity

Calculations of the tacticity of PVC from the infrared spectral data have been performed with the aid of the information from two regions of the spectrum. Germar *et al.*[18)] used the region of the CH_2 scissors to calculate the tacticity from the ratio of the optical densities at 1428 and 1434 cm^{-1}. In the region from 600 to 700 cm^{-1}

the carbon-to-chlorine stretching vibrations absorb. This part of the spectrum is quite complex and an unambiguous assignment of the absorption bands cannot be made: a strong overlap of the bands interferes with this assignment. A detailed discussion of the band assignment will be given in chapter 5.

Most authors obtain the tacticity from the ratio of two absorption peaks but the resulting tacticity values are very uncertain. Their data are shown in table 2.2. and are plotted in figure 2.6. along with the calculated lines from figure 2.7.

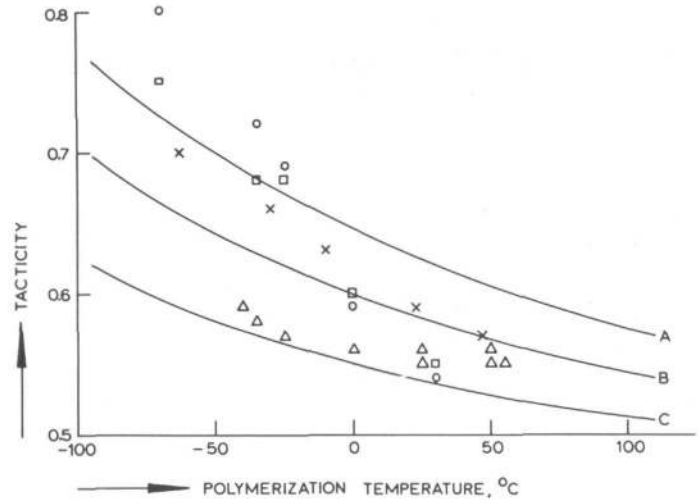

Figure 2.6. Tacticity of PVC as a function of polymerization temperature as measured by IR.

- ○ Germar *et al.*[18)]
- □ Germar[19)]
- △ Stokr *et al.*[20)]
- ✳ Pohl and Hummel[22)]

Table 2.2. Tacticity of PVC as a function of polymerization temperature as measured by IR

Polymerization temperature, °C	Tacticity α	Reference
30	0.54	Germar *et al.*[18]
0	0.59	
- 25	0.69	
- 35	0.72	
- 70	0.80	
30	0.55	Germar[19]
0	0.60	
- 25	0.68	
- 35	0.69	
- 70	0.75	
55	0.55	Stokr *et al.*[20]
50	0.55	
50	0.56	
25	0.55	
25	0.56	
0	0.56	
- 25	0.57	
- 35	0.58	
- 40	0.59	
- 40	0.59	
47	0.57	Pohl and Hummel[21,22]
23	0.59	
- 10	0.63	
- 30	0.66	
- 63	0.70	

2.4. Polymerization temperature and tacticity

The most important factor which influences the tacticity is the polymerization temperature. The reaction rate constants, k_s and k_i, for syndiotactic and isotactic propagation, respectively, are a function of temperature[23,24].

From reaction rate theory we have:

$$k_s = k_s^o \exp(-E_s/RT) \tag{2.1}$$

$$k_i = k_i^o \exp(-E_i/RT) \tag{2.2}$$

hence: $$\frac{k_s}{k_i} = \frac{k_s^o}{k_i^o} \exp(\Delta E/RT) \tag{2.3}$$

Here $$\Delta E = E_i - E_s \tag{2.4}$$

is the difference between the activation energies for isotactic and syndiotactic propagation. The tacticity α can be expressed as

$$\alpha = \frac{k_s}{k_s + k_i} \tag{2.5}$$

This equation combined with equation (2.3) leads to

$$\alpha = \frac{(k_s^o / k_i^o) \exp(\Delta E/RT)}{1 + (k_s^o / k_i^o) \exp(\Delta E/RT)} \tag{2.6}$$

The tacticity as calculated from equation (2.6) is plotted in figure 2.7. for three values of ΔE, combined with three values of the ratio of the frequency factors k_s^o/k_i^o. These values were chosen in such a way that the literature data from IR and NMR measurements fall between the calculated lines (*cf.* figures 2.5. and 2.6.). The difference between the activation energies for isotactic and syndiotactic propagation, ΔE, is thus found to be $\Delta E = (0.45 \pm 0.15)$kcal/mole. It may therefore be concluded that the syndiotactic propagation is indeed only slightly favoured over isotactic propagation.

The tacticity of a commercial atactic PVC produced by polymerization at 40 to 75°C is about 0.55. This value will be used when calculating the crystallinity of atactic PVC.

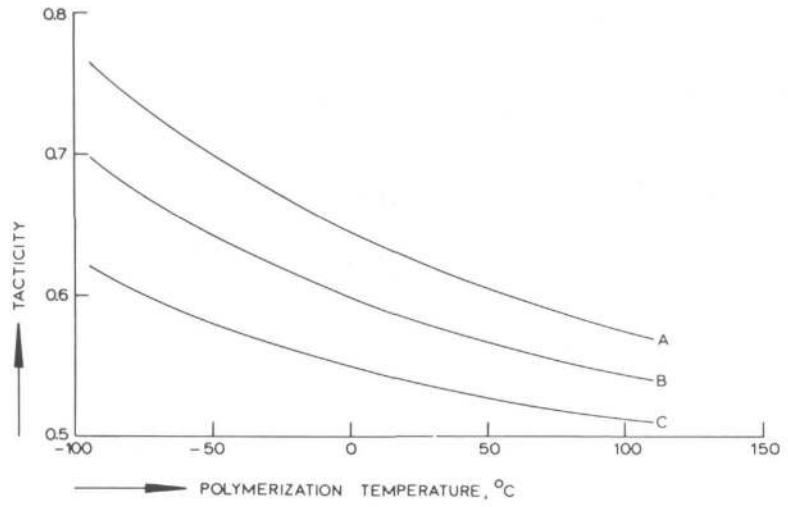

Figure 2.7. Tacticity of PVC as a function of polymerization temperature. Calculation according to equation (2.6).
A: $\Delta E = 0.60$ kcal/mole, $k_s^o/k_i^o = 0.60$
B: $\Delta E = 0.45$ kcal/mole, $k_s^o/k_i^o = 0.65$
C: $\Delta E = 0.30$ kcal/mole, $k_s^o/k_i^o = 0.70$

2.5. Crystallization of an atactic polymer

The chemical structure of the PVC chain is rather regular. Head-to-head and tail-to-tail connections hardly occur and the degree of branching is low. (The chemical structure of PVC is discussed in chapter 5.) Stereochemically, however, the structure is very irregular. As mentioned before, a commercial PVC has a tacticity of about 0.55. This means that such polymers are almost atactic. The irregularity of their stereochemical structure has its consequences for the crystallization of the material.

Several investigators have found that materials of high tacticity show high percentages of crystallinity. This has led to the idea that only the syndiotactic parts in the PVC chains are able to form crystallites. Consequently, many authors consider PVC as a copolymer consisting of a syndiotactic, crystallizable part and an isotactic, non-crystallizable part. On the basis of this assumption it is possible to predict the amount of crystallinity of an atactic PVC. Below, it will be examined whether this theoretical calculation gives the correct value of the crystallinity.

For the crystallization of partly crystallizable copolymers a theory was evolved by Flory[25]. On thermodynamic grounds he derived that the size of crystallites should have a minimum length. Therefore, the parts of the chains contributing to the crystallites should also have that minimum length which is called the minimum sequence length, ξ_{min}.

It is possible to calculate the fraction of total polymer in syndiotactic sequences of length N from the tacticity α. According to Fordham[24]

$$F^{N}_{syndio} = N(1 - \alpha)^{2}\alpha^{N} \qquad (2.7)$$

For a commercial atactic PVC with $\alpha = 0.55$ the sequence distribution is presented in figure 2.8. The fraction of the polymer with a syndiotactic sequence length equal to or larger than N has been derived from this distribution. This enables calculation of the amount of crystallinity that can occur in a polymer if all sequences larger than ξ_{min} contribute to the crystalline phase (figure 2.9). However, as stated by Flory, it is impossible that all sequences of length larger than ξ_{min} contribute to the crystallization. This implies that figure 2.9. represents the maximum amount of the crystalline fraction of the polymer as a function of the minimum sequence length.

With a value of the minimum sequence length, $\xi_{min} = 12$, in agreement with values for other polymers[26], the maximum amount of crystallinity of an atactic PVC ($\alpha = 0.55$) is calculated to be 0.45% (*cf.* figure 2.9). It is a well-established fact that even an atactic PVC crystall-

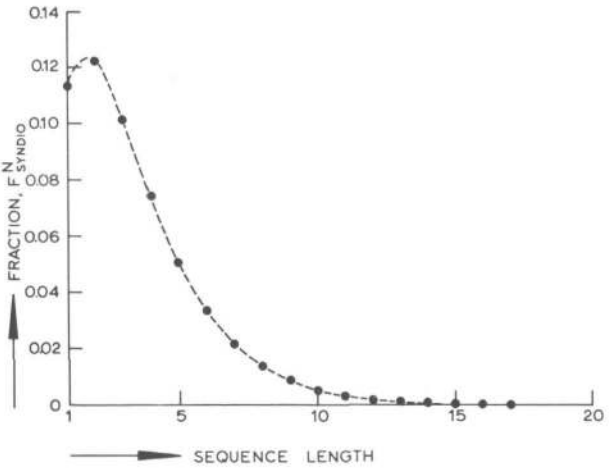

Figure 2.8. Distribution of the sequence length of syndiotactic chain segments for an atactic PVC with $\alpha = 0.55$. Calculation according to equation (2.7).

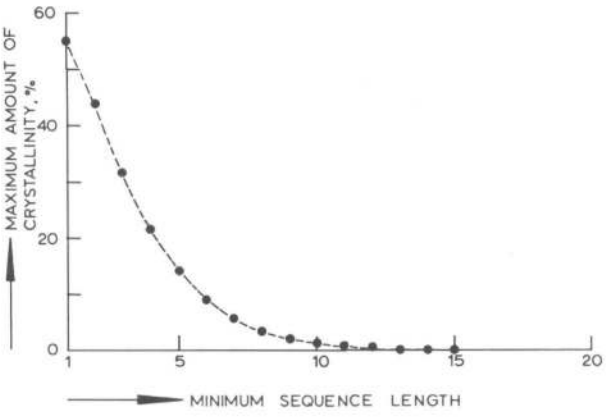

Figure 2.9. Maximum amount of crystallinity for an atactic PVC with $\alpha = 0.55$ as a function of minimum sequence length.

izes to some extent; a crystalline content of about 10% is quite normal. This would correspond to a minimum sequence length of 6 which is an unusually low value for the crystallization of a polymer. The crystallization of such short chain segments results in very small crystallites with large defects at the borders of the crystalline region. However, there are many indications, both from the present experimental work and from literature, that the crystalline structure is much better developed. Therefore it is concluded that the crystallinity of atactic PVC cannot be explained satisfactorily by assuming that only the syndiotactic part of the polymer crystallizes.

2.6. Conclusions

1. The proportion of syndiotactic sequences in the PVC chain increases with decreasing polymerization temperature.
2. The tacticity of PVC can be measured by IR and NMR techniques but the accuracy of these measurements is poor.
3. The observed crystallinity of atactic PVC cannot be explained satisfactorily by assuming that only the syndiotactic part of the polymer crystallizes.

CHAPTER 3

MELTING OF CRYSTALLINITY IN PVC

3.1. Introduction

The crystalline melting phenomena described in this chapter were studied by means of Differential Scanning Calorimetry (DSC). In this type of calorimeter the temperature of a sample and its reference is raised linearly and the difference in heat flows required for the simultaneous temperature increase in measured. The recorder signal gives thermograms in which the glass transition appears as an increase of the heat flux difference whilst melting effects are recorded as endothermic peaks.

Almost similar thermograms are obtained with Differential Thermal Analysis (DTA). However, in DTA the temperature difference between sample and reference is measured as the temperature of both is raised by a constant heat flow. This temperature difference must be converted into a heat flux when, for instance, a heat of fusion has to be calculated from the measurements. In this respect, DSC has an advantage over DTA: the heat flux is measured directly which makes DSC more suitable than DTA for quantitative measurements.

3.2 Equipment and measuring techniques

The calorimetric studies were made with a Perkin Elmer Differential Scanning Calorimeter, type DSC-1B, using polymer samples of 10 - 30 mg. Since the caloric effects associated with melting of crystallites in PVC are small, a high heating rate and a high sensitivity were required. This was attained with a scan speed of $32^{o}C$/min combined with a heat flux range of 4 mcal/sec. At such heating rates the calorimeter has a certain inertia and as a result the measured temperatures are somewhat too high. In order to compensate for this effect to some extent the usual calibration procedure of the apparatus was modified by employing a scan speed of $32^{o}C$/min instead of $8^{o}C$/min. However, there is still

another source of inaccuracy because the calibrations are performed with metals as calibration samples, e.g. indium and tin. These metals have a higher heat conductivity than the polymer samples and it is therefore possible that the measured temperatures are somewhat too high. According to Illers[27] this deviation is 1 - 2°C; a correction for this relatively small error has not been applied in the present work. The cooling rate between successive scans was fixed at 32°C/min except for experiments where the effects on the polymer of slow cooling or quenching were tested.

With a few samples, which were also run in the calorimeter, density measurements were performed in Davenport gradient columns filled with either aqueous zinc chloride or potassium iodide solutions. When potassium iodide was used some sodium thiosulfate (5 g/l) was added to prevent air oxidation of the iodide.

3.3. Materials

The following commercial PVC grades and copolymers of vinyl chloride with vinyl acetate were studied:

1. Corvic D 65/6, suspension PVC, ICI
2. Solvic 239, suspension PVC, Solvay
3. Vestolit E 7001, emulsion PVC, Chemische Werke Hüls
4. Breon 121, emulsion PVC, British Geon
5. Lucovyl RB 8010, bulk PVC, Pechiney - St. Gobain
6. Vinylite VYDR 3, copolymer, 4% vinyl acetate, Union Carbide
7. Solvic 513 PA, copolymer, 13% vinyl acetate, Solvay
8. Vinnol VE 5/65 P, copolymer, 5% vinyl acetate, Wacker Chemie
9. Vinnol E 10/65 P, copolymer, 10% vinyl acetate, Wacker Chemie
10. Vinnol E 15/45, copolymer, 15% vinyl acetate, Wacker Chemie
11. Vinnol VH 13/50, copolymer, 13% vinyl acetate, Wacker Chemie
12. Vinnol H 40/60, copolymer, 40% vinyl acetate, Wacker Chemie
13. Rhodopas AXBM II, copolymer, 17% vinyl acetate, Rhone - Poulenc

In addition, partly syndiotactic PVC's were produced in the laboratory by suspension polymerization at $-30^{o}C$ and $-15^{o}C$. As recommended by Konishi and Nambu [28] a water/methanol mixture (1:1) was used as the continuous phase and the catalyst system lauroyl peroxide/ferrous caproate (both in a concentration of 0.3 mol% on monomer) was employed. The reaction was stopped after five hours by adding oxalic acid or styrene and the polymer purified by dissolution in cyclohexanone and subsequent precipitation in methanol. Since the product obtained in this manner still contained some impurities this procedure was repeated with tetrahydrofuran as the solvent. Finally, the polymer was filtered and washed with methanol and dried for 24 hours at $40^{o}C$ in a vacuum oven.

All the compounds tested were stabilized by adding 3 - 5 %w dibasic lead phosphite.

3.4. Primary crystallinity

Two kinds of crystalline melting effects were found. Primary crystallinity which was detected in virgin PVC is described in this paragraph. Secondary crystallinity induced by annealing the polymer is discussed in the next section.

An example of thermograms obtained with a commercial virgin PVC powder is given in figure 3.1. The samples were tested as received from the suppliers.

The thermograms show a melt region which starts at about $150^{o}C$. The initial melting temperature does not vary significantly among the commercial samples tested, except for Solvic 239 in which melting starts at about $170^{o}C$. Invariably, the melting range extends into the decomposition range. When a virgin PVC powder is heated to a temperature somewhere in the melting range a permanent change is produced in the thermogram: in the subsequent scan the endothermic melting effect commences at the highest temperature that was reached in the first run (*cf.* figure 3.1.), which means that no recrystallization occurs on cooling. In this way, the crystallinity can be removed step by step by successive heat treatments. Similarly, when a PVC compound

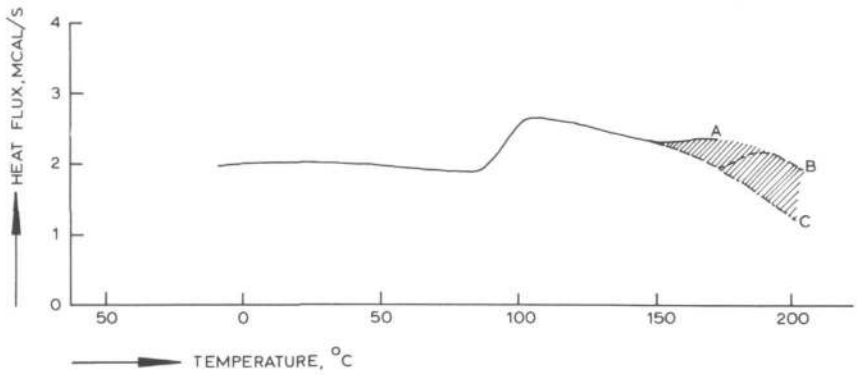

Figure 3.1. Thermograms of commercial PVC; melting of primary crystallinity.

——— first run (A)

— — — second run (B)

—·—·—·— third run (C)

Table 3.1. Melting temperature and melting energy of commercial PVC's.

Polymer grade (see section 3, materials)	Initial melting temperature, °C	Melting energy in the temperature range 150 - 200°C, cal/g
Corvic D 65/6	150	1.2
Solvic 239	170	not measured
Vestolite E 7001	150	1.0
Breon 121	150	1.0
Lucovyl RB 8010	150	1.2
Vinylite VYDR 3 (4% vinyl acetate)	150	small
Other copolymers(> 5% vinyl acetate)	no melting	0

is prepared by milling and pressing, the thermogram clearly shows the highest temperature reached during processing by a steep onset of the endothermic region (thermogram B in figure 3.1.).

Copolymers of vinyl chloride with vinyl acetate behave differently. The copolymer containing 4% vinyl acetate (Vinylite VYDR 3) shows a small melt region whereas in the thermograms of copolymers with a higher vinyl acetate content no melt effect at all can be detected.

The crystalline melting effects are sometimes obscured to some extent by another phenomenon, especially when measurements are performed on PVC powder. When the PVC melts the heat contact between the sample holder and the sample itself improves. As a consequence a smaller heat flux is required temporarily to raise the sample temperature linearly. This change causes a pseudo-exothermic effect in the thermogram almost at the same temperature where the endothermic melting usually starts. To prevent this there should be no change in the heat contact during the scanning of the thermogram. This can be attained by applying a pressure of about 1000 atm when filling the aluminium sample pans which are used in the Perkin Elmer apparatus.

The magnitude of the melt region was estimated by calculating the amount of energy required to melt the crystals present in the polymer in the range between the initial melting temperature and 200°C. The results for a number of commercial samples are listed in table 3.1.

From the above data it is concluded that the differences between the various PVC grades tested are small. Suspension, emulsion and bulk PVC all give the same result. The copolymers show a smaller effect or none at all; apparently, the introduction of vinyl acetate diminishes or prevents crystallization.

Thermograms of the laboratory-prepared, partly syndiotactic PVC polymerized at -30°C are shown in figure 3.2. Here, melting starts at 180°C. The endothermic effect is larger than in commercial polymers. However, the polymer was purified by dissolution and subsequent precipitation. It will be shown below that this procedure causes the crystallinity of the polymer to diminish. Nevertheless, larger

melting effects were found for this polymer than with commercial PVC's, which confirms that its crystallinity is higher.

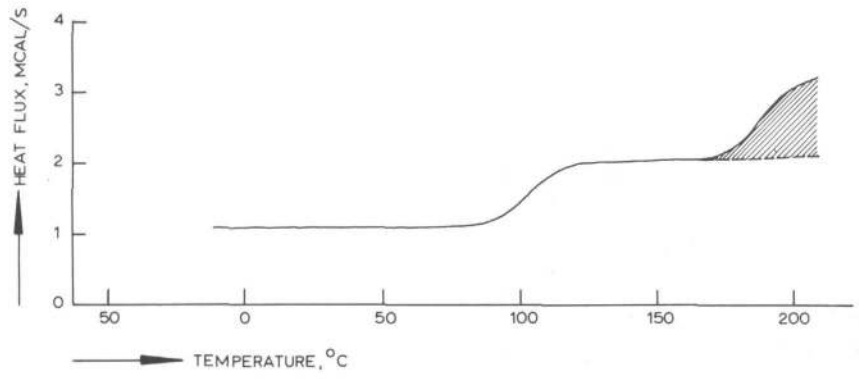

Figure 3.2. Thermograms of PVC polymerized at -30°C; melting of primary crystallinity.

——— first run

– – – – second run

The heat of fusion of the primary crystallinity was found as follows. When samples from a PVC plate are heated up in the calorimeter to 200°C the crystallinity decreases. The heat which is required for the melting was obtained from the thermograms. The decrease in crystallinity was calculated from density measurements on parallel samples. The results of the density measurements are shown in table 3.2.

The densities of entirely syndiotactic (1.44 g/cm^3 [29]) and entirely amorphous PVC (1.41 g/cm^3 [30]) differ by 0.03 g/cm^3. The data of table 3.2. show that the density diminishes by 0.0026 g/cm^3 when heating from 165 to 200°C, which means that the crystalline content diminishes by about 9%. The thermograms reveal that the corresponding melting energy amounts to 1.2 cal/g (table 3.1.). On this basis, a heat of fusion of approximately 13 cal/g or 850 cal/mole of monomer unit is found.

Table 3.2. Densities of commercial PVC samples before and after different heat treatments

Thermal treatment	Density in g/cm^3
Milled and pressed at 165°C	1.4335
Heated at 180°C	1.4325
Heated at 200°C	1.4309

To compare the above result with literature data, values of the (initial) melting temperature and the heat of fusion were collected and listed in table 3.3. The results of the present work agree satisfactorily with those of Kockott[31], Anagnostopoulos *et al.*[34] and Nakajima *et al.*[35], but they differ considerably with the results of other authors using thermal analysis as measuring method. A low melting temperature was reported by Michel[38]; his low value of 114°C can be easily explained, since the experimental work was done with a mixture of PVC and plasticizer which was dry-blended at room temperature. In such a mixture the plasticizer depresses the melting temperature. In the thermograms of Lebedev *et al.*[37] the authors indicate a melting of crystalline structures starting at 200°C. However, the comparison of the thermogram of their initial specimen (A) with that of the sample which they cooled slowly after preheating to 210°C (B) shows an endothermic effect which starts at 150°C and extends into the decomposition range (figure 3.3.). The peak at 200°C may be due to decomposition, since appreciable degradation of the material starts at that temperature when the heating rate is but 4°C/min. The peak at 120°C cannot be explained.

Table 3.3. Melting temperature and heat of fusion of PVC

Melting temperature °C	Heat of fusion cal/mole	Polymer specification	Measuring-method	Reference
150	-	$\alpha = 0.5$	X-ray	Kockott[31]
220	-	$\alpha = 0.8$		
273	2700	$\alpha = 1.0$		
212	-	copolymer with 2-5% vinyl acetate	flow of plasticized PVC	Walter[32]
155	-	$T_{pol} = 125°C$	flow of plasticized PVC	Reding *et al.*[33]
220	-	$T_{pol} = 45°C$		
265	-	$T_{pol} = -10°C$		
> 300	-	$T_{pol} = -80°C$		
174	660	commercial	polymer-diluent	Anagnastopoulos *et al.*[34]
285	785	$T_{pol} = -15°C$	polymer-diluent	Nakajima *et al.*[35]
310	785	$T_{pol} = -75°C$		
225	-	commercial	DTA	Clark[36]
200(150)	-	commercial	DTA	Lebedev *et al.*[37]
114	-	commercial PVC plasticized	DTA	Michel[30]
150	750*)	commercial	DSC	Juijn *et al.*[39]
180	-	$T_{pol} = -30°C$		

*) In this thesis the value of the heat of fusion was recalculated to be 850 cal/mole.

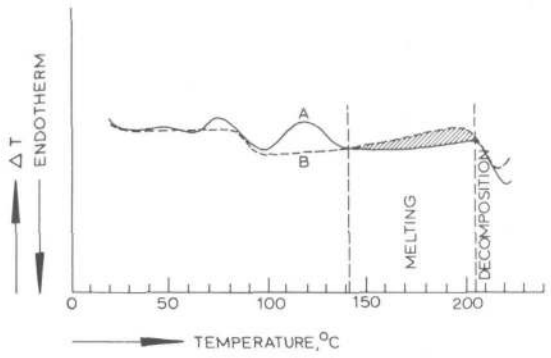

Figure 3.3. Thermograms of PVC produced at 50°C: A - initial specimen; B - the same specimen cooled slowly from 210 to -70°C. (According to Lebedev *et al.*[34])

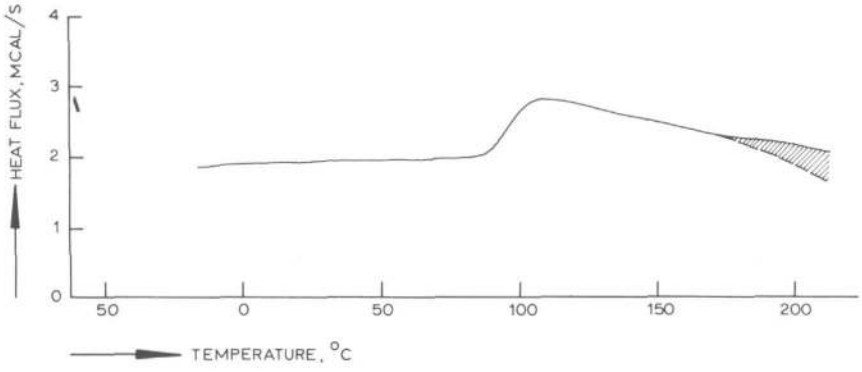

Figure 3.4. Thermograms of commercial PVC slowly precipitated from tetrahydrofuran.
——— first run
– – – – second run

The thermograms in figure 3.1. show that the primary crystallinity is removed partially by heating to a temperature in the melting range. Once this crystallinity has disappeared it is very difficult to restore it. A successful method for recrystallization of the polymer is slow and careful precipitation from solution. To this end the polymer is dissolved in tetrahydrofuran (2 % w solution) and methanol is then

slowly added to this solution whilst stirring vigorously. The powder obtained in this way contains crystallinity (see figure 3.4.). On the other hand, entirely amorphous PVC is obtained by 'quick' precipitation, when the PVC solution is added to the methanol. In that case no endothermic effects are found in the thermogram.

3.5. Secondary crystallinity

We have seen that recrystallization of the primary crystallinity is impossible. However, annealing at a temperature above the glass transition temperature does produce some crystalline order in preheated polymer. This follows from figure 3.5., in which thermograms are shown of a commercial PVC powder which was annealed at 100°C. An endothermic region is formed adjacent to the annealing temperature. The maximum of this endothermic peak is located at T_{max}.

The original melting range (primary crystallinity) is never entirely restored, not even after prolonged annealing. The thermograms of figure 3.5. show that the annealing effect is eliminated by subsequent heating; it does not reappear unless the polymer is again annealed.

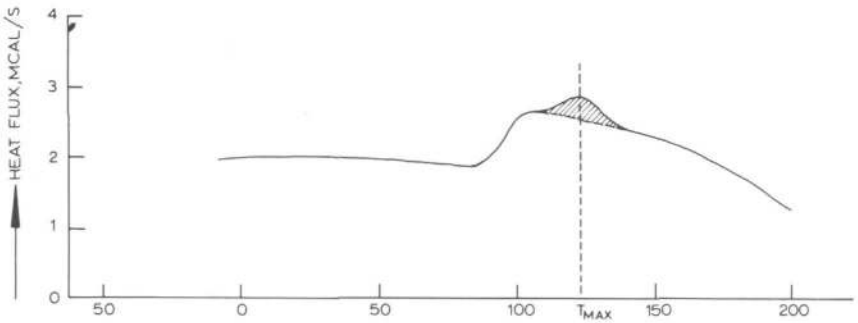

Figure 3.5. Thermograms of commercial PVC; annealing at 100°C.

——— first run

— — — second run

Annealing experiments were performed at various temperatures between the glass transition temperature and the decomposition range. Samples which were preheated at 180°C were annealed for 16 hours. The results, shown in figure 3.6., indicate that there is a maximum annealing effect at about 110°C.

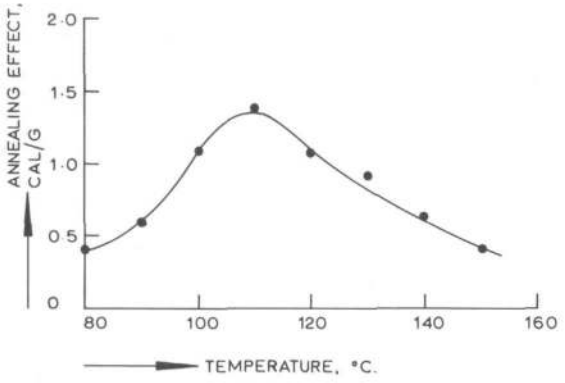

Figure 3.6. Influence of annealing temperature on the magnitude of the annealing effect (annealing for 16 hrs).

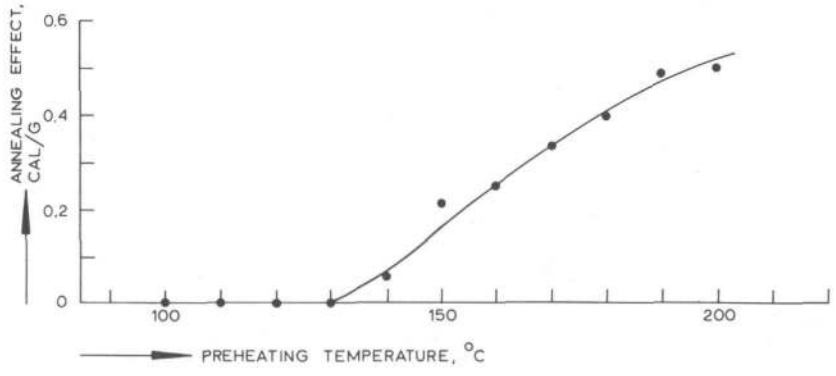

Figure 3.7. Influence of preheating temperature on the magnitude of the annealing effect (annealing for 0.5 hr at 100°C).

The magnitude of the annealing effect depends on the extent to which the primary crystallinity has been melted by prior heating. The effect becomes larger when the amount of primary crystallinity left after preheating decreases. An untreated virgin powder does not show any effect at all (see figure 3.7.).

The annealing effect increases in intensity when annealing is prolonged. This is shown in figure 3.8. Moreover, figure 3.9. shows that the newly formed melting range then shifts to a higher temperature. These results indicate that the secondary crystalline order induced by annealing becomes more extensive and increasingly perfect at longer annealing times.

Secondary crystallinity is formed in all kinds of commercial PVC and also in syndiotactic PVC. However, the copolymers containing vinyl acetate behave differently. In figure 3.10. the annealing effect for various copolymers is compared with that of the homopolymer (Solvic 239). There is a gradual decrease of the annealing effect when the vinyl acetate content of the copolymer increases; at 40% vinyl acetate secondary crystallinity is not formed at all. This is in contrast with the influence of comonomers on the formation of primary crystallinity; as was shown previously a small vinyl acetate content (5%) entirely prevents the formation of primary crystallinity.

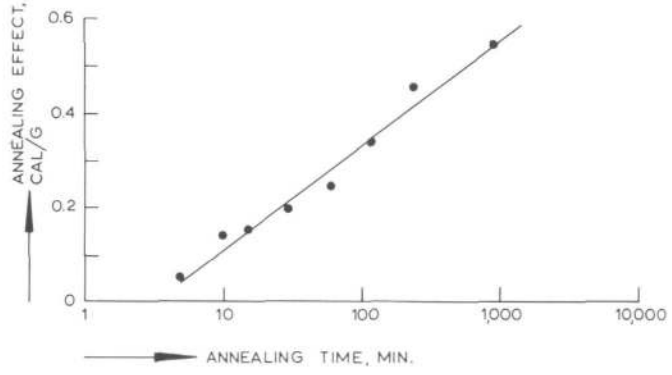

Figure 3.8. Influence of annealing time on the magnitude of the annealing effect (annealing at 100°C, preheating temperature 165°C).

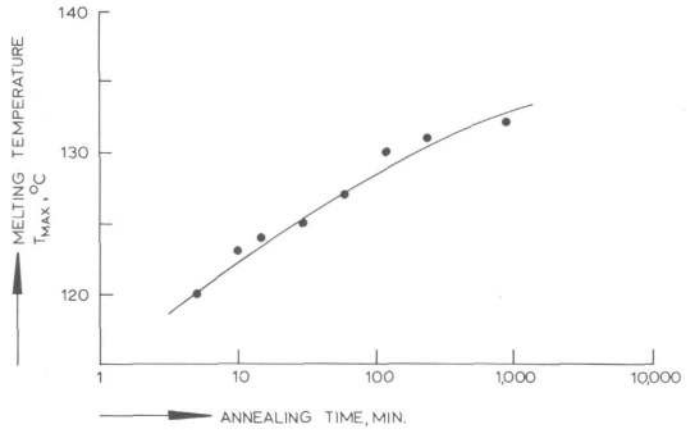

Figure 3.9. Influence of the annealing time on the melting temperature of the induced structures (annealing at 100°C, preheating temperature 165°C).

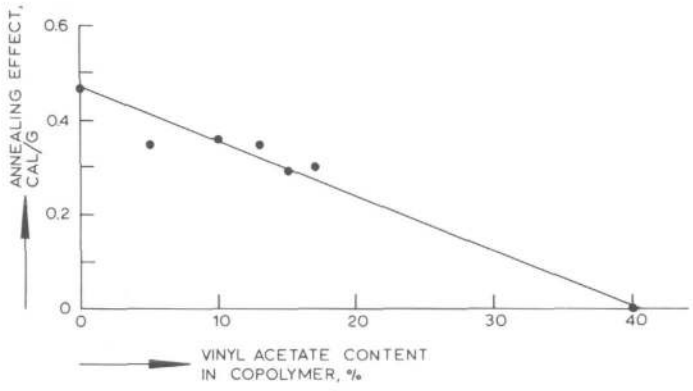

Figure 3.10. Influence of vinyl acetate content in copolymer on the magnitude of the annealing effect (annealing for 1 hr at 100°C, preheating temperature 200°C).

The procedure for the estimation of the heat of fusion of the secondary crystallinity is similar to that applied to the primary crystallinity described in the previous section. Again, the density difference and the thermal effect were measured with the same samples.

The results of the measurements on samples of commercial PVC before and after annealing are listed in table 3.4. The density values are plotted as a function of the annealing effect in figure 3.11. A density difference of 0.022 g/cm^3 is measured when the annealing effect amounts to 0.5 cal/g. From these data a heat of fusion of about 400 cal/mole is calculated assuming that a material having 100% secondary crystallinity has the same density as a material of 100% primary crystallinity.

3.6. Annealing below the glass transition temperature and quenching

In literature reports many authors mention crystalline phenomena occuring in or just above the glass transition region. The effects arise when a sample of PVC is annealed at a temperature just below the glass transition region and when a sample is quenched from a high temperature (approximately 200°C) to a low temperature[27,40,41,42]. In figure 3.12. these effects are shown. Curve A represents a normal DSC thermogram. Curve B shows an endothermic effect for an annealed sample; similar thermograms are found when a sample is slowly cooled from a temperature above the glass transition[27,43]. The exothermic effect in curve C is caused by quenching.

Both these thermal effects have been ascribed to crystalline phenomena:[40,41,42] the annealing peak has been attributed to the melting of structurally ordered material and the exothermic quench peak was interpreted as crystallization. The explanations must be incorrect since the two effects can be obtained with various kinds of polymers, whether they are crystalline, semi-crystalline or amorphous. PVC, copolymers of vinyl chloride and vinyl acetate, polyvinyl acetate[44], polystyrene[45] all behave in this manner. Although polystyrene contains neither primary nor secondary crystallinity and thus is completely amorphous, it nevertheless shows the glass transition effects discussed here.

The correct explanation for these effects is enthalpy relaxation[40, 44-49]. Figure 3.13. (according to Wilski[40]) shows the enthalpy-temperature relationship. After quenching the enthalpy of the polymer

Table 3.4. Densities of commercial PVC samples before and after annealing

Thermal treatment	Annealing time, min	Annealing effect, cal/g	Density, g/cm^3
Preheated at 180°C	0	0	1.4334
Preheated at 180°C annealed at 100°C for:	5	0.05	1.4337
	10	0.14	1.4339
	15	0.15	1.4340
	30	0.20	1.4343
	60	0.25	1.4349
	120	0.34	1.4348
	240	0.44	1.4355
	900	0.52	1.4357

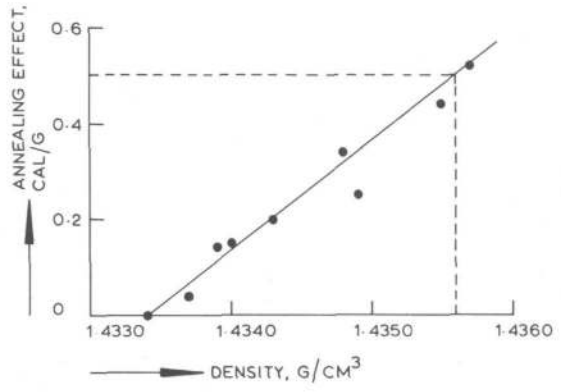

Figure 3.11. Density as a function of the magnitude of the annealing effect (annealing at 100°C, preheating temperature 180°C).

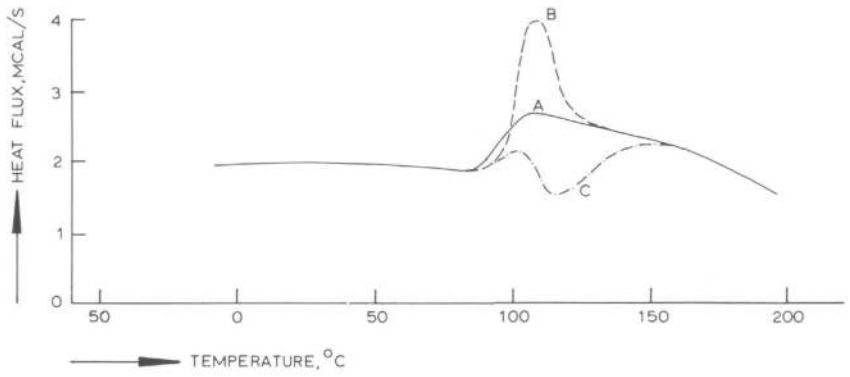

Figure 3.12. Thermograms of commercial PVC; glass transition effects.

——— normal thermogram (A)

– – – – thermogram after annealing below the glass transition temperature (B)

—·—·— thermogram after quenching (C)

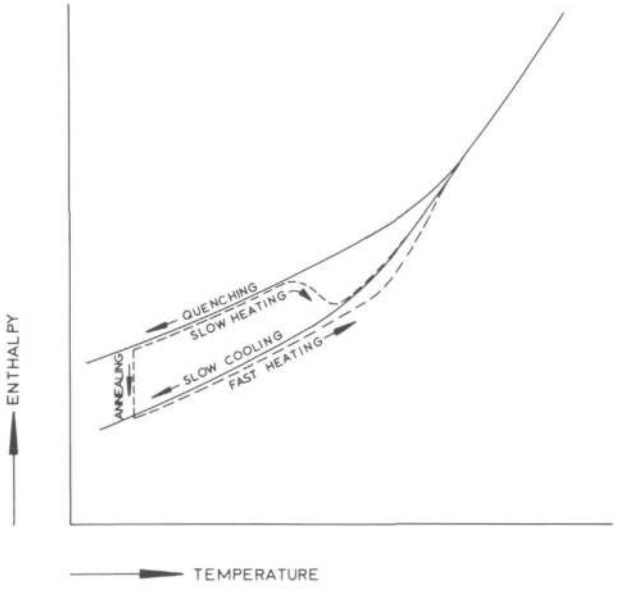

Figure 3.13. Enthalpy-temperature relation in the glass transition region. (According to Wilski[37]).

is too high and therefore subsequent slow heating gives a drop in enthalpy in the glass transition region which is observed as an exothermic peak in a DSC thermogram. Conversely, annealing in the glass region or slow cooling of a sample causes the enthalpy to reach a low level. In that case a high heating rate produces an endothermic effect in the thermogram. Such enthalpy curves were measured by Sharonov and Volkenshtein[45] for polystyrene. It was thus shown that these so-called crystalline effects are actually relaxation phenoma.

3.7. Conclusions

1. Two types of crystallinity can exist in PVC:
   a. Primary crystallinity of relatively high order, which occurs in virgin powder.
   b. Secondary crystallinity having a lower degree of order, which results from annealing when the primary crystallinity has wholly or partly been melted.
2. The thermal effects in or just above the glass transition region which are caused by annealing below the glass transition temperature and quenching are relaxation phenomena.

CHAPTER 4

AGING OF PLASTICIZED PVC

4.1. Introduction

Objects made of plasticized PVC stiffen in the course of time. So far, this phenomenon has not been explained satisfactorily and only few data have been published on the aging of technically and economically important plasticized compounds containing PVC. A RAPRA-report[50] attributes the aging to segregation of polymer and plasticizer. A similar"stiffening" is observed when aging PVC in solution[51,52] and soft PVC gels[53,54]. In these cases the formation of supramolecular structures is held responsible for the aging.

When PVC is plasticized the glass transition temperature decreases. A compound with about 25 % w of plasticizer has a glass transition temperature below room temperature. Since annealing of rigid PVC above the glass transition temperature causes secondary crystallinity it is logical to assume that crystallization proceeds to some extent in plasticized compounds during storage at room temperature. Below, the hypothesis that crystallization causes the aging of these materials is examined experimentally.

4.2. Equipment and measuring techniques

The calorimetric studies and density measurements were carried out as described in chapter 3, section 2. Moduli of elasticity were measured on an Instron Universal Testing Instrument, floor model (TT-CM). Polymer samples with a cross section of 1 x 0.2 cm and a length between the clamps of 8 cm were tested at a strain rate of 0.5 cm/min. The modulus of elasticity at 0.5% relative strain was calculated from the stress-strain diagram.

4.3. Materials

The following commercial polymers were studied in plasticized compounds:

1. Corvic D 65/6, suspension PVC, ICI
2. Solvic 239, suspension PVC, Solvay
3. Vestolit E 7001, emulsion PVC, Chemische Werke Hüls
4. Carina 16 F, emulsion PVC, Shell
5. Vinylite VYDR 3, copolymer, 4% vinyl acetate, Union Carbide
6. Solvic 513 PA, copolymer, 13% vinyl acetate, Solvay
7. Haloflex 243, chlorinated polyethylene containing 43% chlorine, ICI
8. $-15^{o}C$ polymerizate, see chapter 3, section 3

The following plasticizers were used in the compounds:

1. Scadoplast 8 P, di-2-aethylhexyl phtalate (DOP), Scado-Archer-Daniels
2. Tricresylphosphate (TCP), U.C.B.
3. Scadoplast 8 A, di-octyl adipate (DOA), Scado-Archer-Daniels
4. Scadoplast W 2, polyester from phtalic acid, Scado-Archer-Daniels
5. Scadoplast RA 5, polyester from adipic acid, Scado-Archer-Daniels
6. Cereclor S 52, chlorinated paraffine containing 52 % w chlorine, ICI

All compounds were stabilized with 2 % w dibutyl tin dilaurate and 0.5 % w zinc stearate.

4.4. Annealing of plasticized PVC

Thermograms were recorded on samples of plasticized PVC compounds containing 30 parts by weight of DOP per 100 parts of PVC. The test samples had been stored at room temperature for varying periods of time. An example of the results is shown in figure 4.1.; secondary crystallinity is clearly shown by the thermograms.

The glass transition temperature is situated below room temperature. This means that storage at room temperature is, for this material,

equivalent to annealing it above the glass transition. The same phenomenon observed when annealing rigid PVC is thus found here for the plasticized compounds: secondary crystallinity is formed in increasing amounts as the time of storage is longer. Also, the melting range then shifts to higher temperature. Concomitantly, the modulus of elasticity of the material increases (see figure 4.2.) and the same applies to the density of the compound[55] (figure 4.3.).

For all the polymers studied -including the low temperature polymerizate, the copolymers and the chlorinated polyethylene- similar results were obtained. This is illustrated by an extensive comparison of the stiffening of various compounds at the end of this section.

The formation of secondary crystallinity in plasticized PVC is a reversible process. Reheating to 80°C causes the crystalline order to disappear; simulteanously, the modulus of elasticity decreases to the value which was found right after processing of the compound. The phenomena studied here have sometimes been ascribed to loss of plasticizer by evaporation, but this is disproved by chemical analysis.

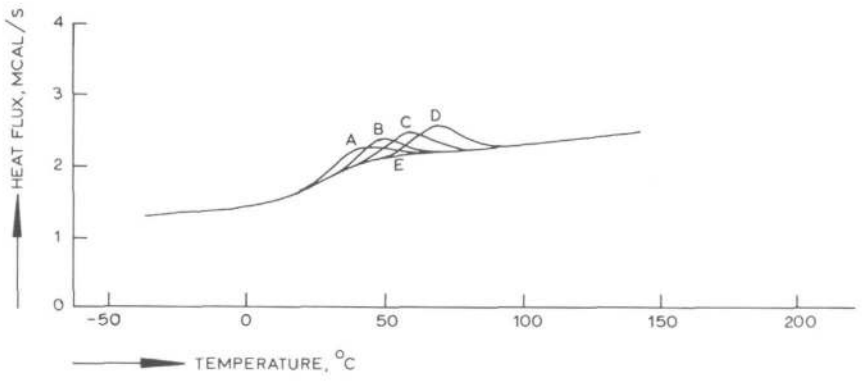

Figure 4.1. Thermograms of plasticized PVC containing 30 parts of DOP on 100 parts of PVC; annealing effect obtained by storage at room temperature for
A: 0.5 h, B: 18 h, C: 10 days, D: 0.5 year.
E: without annealing.

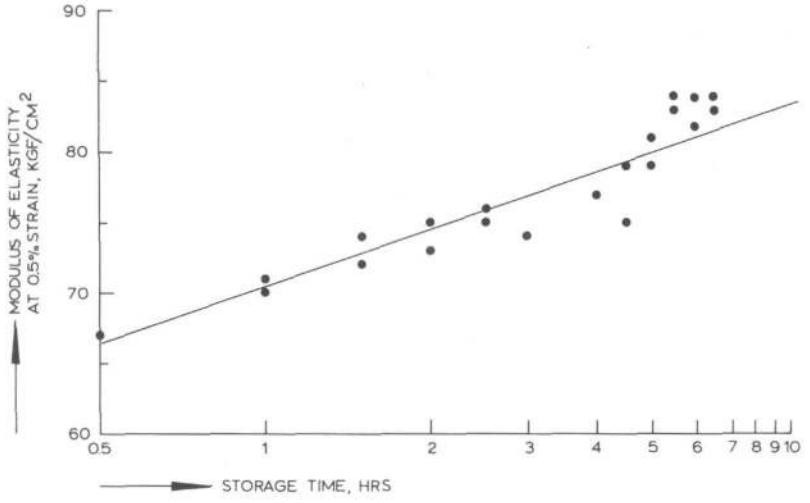

Figure 4.2. Influence of storage time on the modulus of elasticity for plasticized PVC containing 30 parts of DOP on 100 parts of PVC. Storage and measurement of modulus at room temperature.

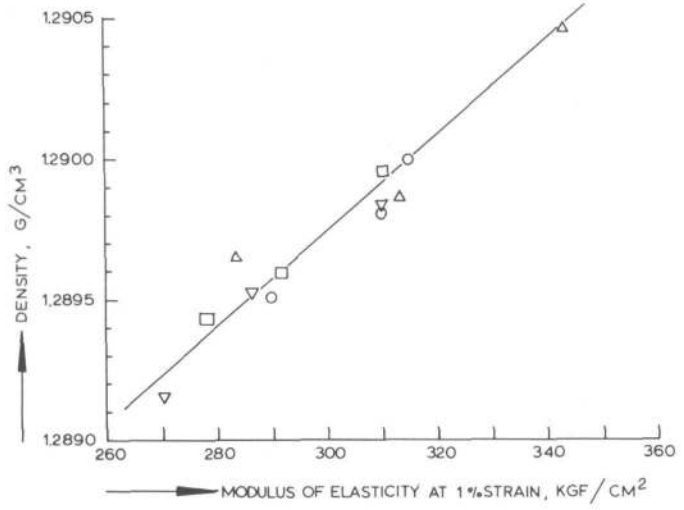

Figure 4.3. Relation between modulus of elasticity and density of plasticized PVC containing 27.6% DOP. Increase of modulus of elasticity and density obtained by storage at room temperature (According to Gisolf[55]).

Another theory based on the segregation of plasticizer and PVC[50] is incompatible with the fact that compounds with all kinds of plasticizer, including polymeric plasticizers, show aging. Even the chlorinated polyethylene, without plasticizer, shows an increasing stiffness in the course of time. The increase in the moduli of the plasticized material should therefore be ascribed to the formation of secondary crystallinity. This is in line with the theory of several authors, *viz.* that the rubberelastic behaviour of plasticized PVC may be attributed to physical crosslinking caused by crystallites[53,55]. It also explains that the aging process is reversible: upon heating the annealing structures are melted.

Aging of plasticized PVC at room temperature is similar to aging of pure PVC at a temperature above the glass transition region. When PVC is annealed at 100°C and the modulus of elasticity is measured at that same temperature an increase in stiffness is observed. This is shown in figure 4.4. which closely resembles the aging of plasticized PVC presented in figure 4.2.

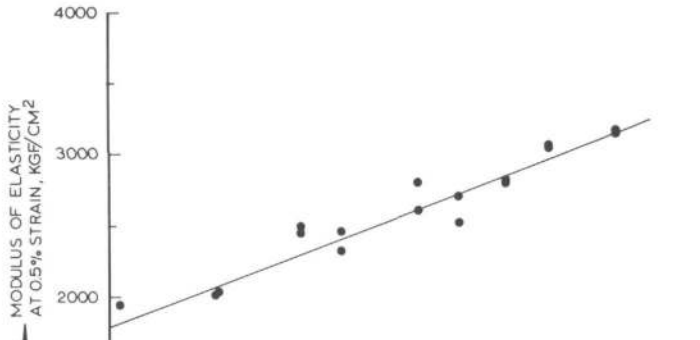

Figure 4.4. Influence of storage time on the modulus of elasticity of unplasticized PVC (Solvic 239). Storage and measurement of modulus at 100°C.

The increase of the modulus of elasticity was determined for a large variety of plasticized compounds. From plots like that of figure 4.2. the moduli of elasticity at 1 hour and 1000 hours were taken (E_1 and E_{1000}, respectively). The ratio of these values, E_{1000}/E_1, is a measure of the rate of aging of the compound. The experimental results are listed in table 4.1.

The rate of aging, E_{1000}/E_1, is plotted as a function of the modulus of elasticity, E_1, in figure 4.5. The aging is accelerated by lowering the stiffness of the compound. It is considered significant that all the compounds tested fit in the same curve: it means that compounds containing the partly syndiotactic polymer, the copolymers and even the chlorinated polyethylene most probably produce the same type of crystallinity as the commercial PVC compounds.

The above findings lead to a general conclusion which is important in applications, *viz.* that it will be very difficult to prevent the aging of plasticized compounds. The structures formed upon aging have such a low degree of order that the introduction of defects in the chain does not help to prevent their being formed. Changing the type of plasticizer is equally without effect.

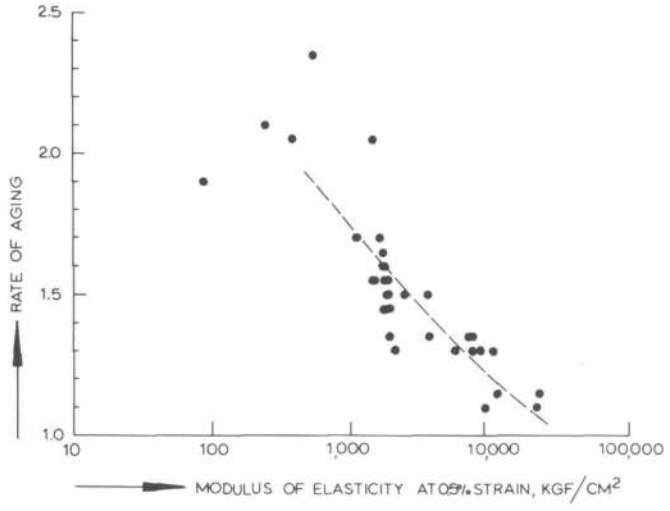

Figure 4.5. Aging of plasticized PVC compounds as a function of the modulus of elasticity.

Table 4.1. Aging of plasticized PVC. Measurement of modulus elasticity

Polymer	Plasticizer	Amount of plasticizer, parts/100 parts of PVC	Press temperature °C	E_1 kgf/cm^2	E_{1000} kgf/cm^2	E_{1000}/E_1, rate of aging
Corvic D 65/6	Scadoplast 8P	30	165	1720	2500	1.45
Corvic D 65/6	Scadoplast 8P	30	165	1800	2900	1.60
Corvic D 65/6	Scadoplast 8P	30	165	1820	2650	1.45
Corvic D 65/6	Scadoplast 8P	30	165	1850	2800	1.50
Corvic D 65/6	Scadoplast 8P	30	165	1900	2860	1.50
Corvic D 65/6	Scadoplast 8P	30	165	1930	2640	1.35
Corvic D 65/6	Scadoplast 8P	30	165	1940	2800	1.45
Corvic D 65/6	Scadoplast 8P	30	165	2100	2760	1.30
Corvic D 65/6	Scadoplast 8P	30	185	1750	2750	1.55
Corvic D 65/6	Scadoplast 8P	26	165	3600	5500	1.50
Corvic D 65/6	Tricresylphosphate	30	165	9350	10500	1.10
Corvic D 65/6	Scadoplast 8A	30	165	540	1270	2.35
Corvic D 65/6	Scadoplast W2	30	165	5700	7300	1.30
Corvic D 65/6	Scadoplast W2	33	165	3700	5000	1.35
Corvic D 65/6	Scadoplast W2	40	165	1100	1850	1.70
Corvic D 65/6	Scadoplast RA5	30	165	7600	9250	1.35
Corvic D 65/6	Cereclor S52	30	165	8650	11100	1.30

Table 4.1. continued

Polymer	Plasticizer	Amount of plasticizer, parts/100 parts of PVC	Press temperature °C	E_1 kgf/cm^2	E_{1000} kgf/cm^2	E_{1000}/E_1, rate of aging
Solvic 239	Scadoplast 8P	30	165	1720	2860	1.65
Vestolit E 7001	Scadoplast 8P	30	165	1500	2350	1.55
Carina 16F	Scadoplast 8P	30	165	1420	2220	1.55
Vinylite VYDR 3	Scadoplast 8P	30	165	1600	2700	1.70
Vinylite VYDR 3	Scadoplast 8P	30	140	1780	2800	1.55
Vinylite VYDR 3	Scadoplast 8P	20	150	10500	13800	1.30
Solvic 513 PA	Scadoplast 8P	30	110	380	780	2.05
Solvic 513 PA	Scadoplast 8P	20	100	7100	9700	1.35
Haloflex 243	Scadoplast 8P	5	165	1450	2950	2.05
Haloflex 243	-	-	165	7600	10100	1.30
-15°C polymerizate	Scadoplast 8P	30	165	2400	3550	1.50
Solvic 239	Scadoplast 8P	0	160	22000	24400	1.10
Solvic 239	Scadoplast 8P	10	160	22500	25600	1.15
Solvic 239	Scadoplast 8P	20	160	11300	13200	1.15
Solvic 239	Scadoplast 8P	30	160	1760	2580	1.45
Solvic 239	Scadoplast 8P	40	160	240	500	2.10
Solvic 239	Scadoplast 8P	50	160	86	162	1.90

4.5. Conclusions

1. Secondary crystallinity is formed in plasticized PVC during storage at room temperature.
2. The formation of such structures accounts for the stiffening of plasticized compounds in the course of time.
3. Aging occurs with various kinds of plasticizer.
4. The aging process is independent of the syndiotacticity of the PVC and also occurs in copolymers of vinyl chloride with vinyl acetate and even in a highly chlorinated polyethylene.

CHAPTER 5

CHAIN STRUCTURE

5.1. Chemical and stereochemical structure of the chain

In the previous chapters it has been pointed out that atactic PVC crystallizes to some extent. Since crystalline order in a polymeric material requires strict regularity of the chains, the question arises how and to what extent even atactic PVC can still be packed in a regular crystal lattice. Chain regularity is determined by its chemical structure (chemical impurities, branching, head-to-tail structure) and its stereochemical structure (configuration, conformation). These subjects will be discussed in this chapter.

Chemical impurities may be incorporated in the chain during polymerization. Many of these are attached to the chain ends, e.g. as initiator groups. However, there is a high level of chain transfer during the polymerization of vinyl chloride. This means that a large fraction of the molecules is started through transfer reactions and, consequently, many molecules do not contain initiator groups. This was shown by Razuvayev *et al.*[56], who found only 0.19 to 0.40 initiator groups per molecule. The molecules which were started through transfer reaction contain olefinic end groups with almost the same size as the monomer unit. Hence, the effect of chemical impurities on the regularity of the chain is likely to be of minor importance.

Another factor causing irregular chain structure is branching. The measurement of the degree of branching is very laborious: the polyvinyl chloride is first reduced by lithium aluminium hydride to polyethylene and then the content of methyl groups of this polyethylene is estimated by infrared analysis[35,57]. The method does not reveal the length of the branches: each branch, whether short or long, is counted as one side chain. At best, the results are semi-quentative. The degree of branching is usually given as the methyl content of the

reduced PVC ($CH_3/100CH_2$). For commercial PVC's values of 0.2[35], less than 0.5[58], 0.4 to 1.1[57], 1.6[59] and 1.5 to 1,8[60] have been reported. From these figures we conclude that branching is not the major factor that determines the crystallinity of PVC.

The third phenomenon which contributes to the chemical structure of the chain is the manner in which monomer is added during the growth of the chain. The monomer unit in the chain consists of two groups, *viz.* the CHCl group and the CH_2 group. These groups can be called the head and the tail of the monomer, respectively. Thus, the propagation step in the formation of PVC can yield a head-to-tail, a head-to-head and a tail-to-tail addition. It was shown by Marvel *et al.*[61] that head-to-tail addition of the monomer occurs far more readily than head-to-head or tail-to-tail addition. Fierz-David and Zollinger[62] estimated the proportion of irregular monomer additions to be less than 1.5%. From this low figure it is concluded that head-to-head and tail-to-tail structures are not likely to prevent the crystallization of PVC.

Since the content of chemical impurities, degree of branching and the amount of irregular monomer addition are low, the structure of the chain is determined almost exclusively by stereochemical factors. For a vinyl polymer like PVC two factors should be considered:

1. The stereoregularity of the chain (configuration)
2. The spatial arrangement of the chain backbone (conformation).

In this investigation, the use of atomic models proved to be a very suitable means of studying the stereochemical structure of PVC. New Courteauld Atomic Models were used, which have dimensions corresponding to the following values of atomic distances: d_{CC} = 1.54 A, d_{CH} = 1.07 A and d_{CCl} = 1.76 A. In a Table of Selected Bond Lengths, published by the Chemical Society[63], average values of these bond lengths are listed as follows:
d_{CC} = (1.537 $\pm$ 0.005)A, d_{CH} = (1.096 $\pm$ 0.005)A and d_{CCl} = (1.767 $\pm$ 0.005)A. Besides, all valence angles in the PVC chain are very close to the valence angle of tetrahedral carbon. Since this also holds for the Courteauld models they are regarded as adequately realistic.

5.2. Nomenclature

For a unique description of the chain structure the configuration and conformation parameters have to be defined first. There is no system which is generally used in literature, but this is not a serious problem because it is quite easy to translate the symbols of one nomenclature into the symbols of any other system. Our nomenclature can be illustrated by means of the Newman projection of the chain (see chapter 2.1.). If two atoms have the same projection they are distinguished by indicating the atom lying in front by a point and the rear atom by a circle. As direction of projection the C-C bond in the monomer was chosen, with the CH_2 group lying in front of the CHCl group. (see figure 2.3.)

5.2.1. Configuration parameters

A monomer unit in the chain can be right-handed (R) or left-handed (L) as defined in chapter 2.1. Here, figure 2.3. is reproduced again to show the Newman projections of the (R) and (L) monomer unit.

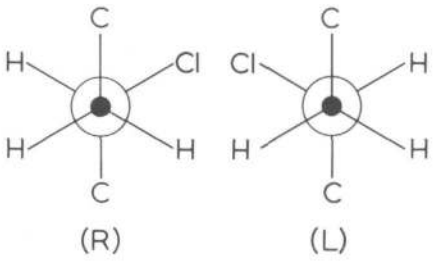

Figure 2.3. Newman projections of the right-handed and left-handed monomer unit.

5.2.2. Conformation parameters

A carbon-to-carbon bond in the chain can be trans, gauche-right or gauche-left. The Newman projections of figure 5.1. are used to define the symbols T, G_r and G_l.

There is a C-C bond coming into and a C-C bond going out of the monomer. The C-C bond of the monomer is called *trans*, T, if the two C-C bonds, coming in and going out, are parallel. The bond is called *gauche-right*, G_r, when the incoming bond can be made parallel with the outgoing bond by a clockwise rotation over 120^{o}. Similarly, a bond is named *gauche-left*, G_l, when the rotation is counter-clockwise. These three conformations around the C-C bond are called the staggered positions. The eclipsed positions have a higher energy since they are situated at potential barriers. Therefore only the staggered conformations will be considered.

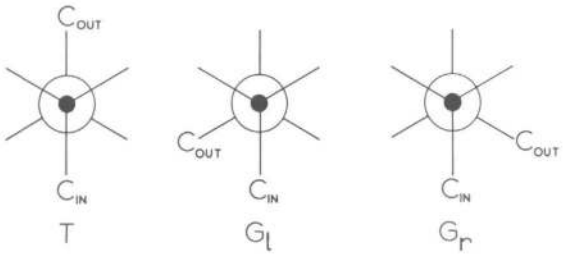

Figure 5.1. Newman projections of the three different conformations around a C-C bond.

5.3. Conformation

5.3.1. Monomer conformations

A monomer unit is fully characterized by combining one configuration parameter with one conformation parameter. Each configuration parameter (R and L) can be combined with every conformation parameter (T, G_l, G_r). This results in six possible different representations of the monomer unit, (TR), (G_rR), (G_lR), and their mirror images, (TL), (G_lL) and (G_rL), respectively. The combination of symbols is placed in brackets; this means that it indicates a monomer unit. The Newman projections of the six monomer conformations are given in figure 5.2.

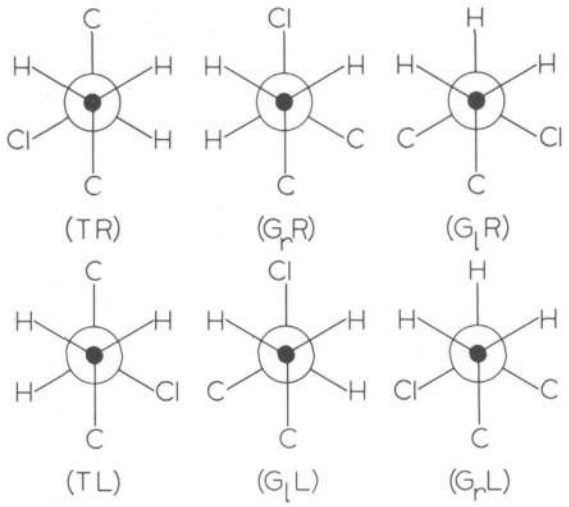

Figure 5.2. Newman projections of the six monomer conformations.

5.3.2. Pair conformations

The first step in building the PVC chain from atomic models is to assemble the monomer unit of which six different conformations exist (see above). These monomer units are then combined into pairs. On paper every conformational form of both monomer units can be combined with any other form of the monomer in three different ways: T, G_r and G_l. We are thus led to expect 6 x 6 x 3 = 108 different pair conformations.

However, steric hindrance markedly reduces the number of pair conformations. The pair conformations which are excluded can be divided into two groups. The first group consists of pairs which cannot be constructed because of internal steric hindrance. A good example of this class is the all-trans isotactic pair (TR)T(TR) or (TL)T(TL). Here the chlorine atoms are contiguous and the construction of this pair with atomic models is impossible. The second group

is excluded because of external steric hindrance. Here the pair as such is without steric hindrance, but it is not possible to attach a third monomer, whether in front of or behind the pair.

Table 5.1. Conformations of pairs of monomer units.
(All mirror image conformations have been omitted)

Classification	Syndiotactic	Isotactic
trans without steric hindrance	(TR)T(TL) (G_lR)G_l(G_lL)	(TR)G_l(TR) (G_lR)T(G_rR)
trans with some steric hindrance	(TR)G_l(TL) (G_rR)G_r(G_rL) (G_rR)T(G_lL)	(TR)G_r(TR) (G_rR)G_r(G_rR) (G_rR)T(G_lR) (G_lR)G_l(G_lR)
gauche without steric hindrance	(TR)G_l(G_lL) (G_rR)T(TL) (G_lR)T(TL)	(TR)T(G_rR) (G_rR)T(G_rR) (G_lR)G_l(TR)
gauche with some steric hindrance	(TR)G_r(G_rL) (TR)T(G_lL) (G_lR)G_l(TL) (G_lR)T(G_lL)	(TR)G_r(G_rR) (TR)T(G_lR) (TR)G_l(G_lR) (G_rR)G_r(TR) (G_lR)T(G_lR)

Table 5.1. lists the pairs of monomer units with no or only a limited amount of steric hindrance. Every pair that can be constructed from New Courteauld Atomic Models without breaking bonds is mentioned in this tabel. The pairs are classified as follows:

1. A pair can be syndiotactic or isotactic. As was stated in chapter 2, combinations (R)(L) and (L)(R) are syndiotactic, (R)(R) and (L)(L) isotactic.
2. A pair can be trans or gauche. In the previous section a monomer was defined as trans when the two vicinal C-C bonds around the central C-C bond of the monomer are parallel. The same applies to the pair. When the C-C bonds coming into the pair and that going out of the pair are parallel the pair is called trans. Gauche pairs can be defined similarly.
3. Some steric hindrance was allowed in constructing the pairs. As a consequence, there are classes of pairs with and without some steric hindrance.

5.3.3. Chain conformations

Now that all possible pair conformations are known the third step in building the chain can be made: combining pairs of monomer units. This is not always possible. If a pair A-B is combined with a pair C-D, forming a part of the chain A-B-C-D, we have to check that the pair B-C is allowed. This technique yields a large number of chain conformations. Here, the basic question of this thesis (chapter 1) should be remembered, *viz.* to explain the occurrence of crystallinity in atactic PVC. Crystallization of a polymer requires straight chain conformations of the molecules and therefore, only these conformations will be studied below.

PVC crystallinity was first described by Natta and Corradini[29] when reporting the results of their X-ray measurements on atactic PVC. They concluded that PVC crystallizes in an orthothombic lattice and considered this to be the crystal form of pure syndiotactic chains with a planar zig-zag conformation. In the second chapter it was shown that in atactic PVC a crystalline content of about 10% cannot be formed from the syndiotactic chain segments only. Obviously, other straight chain conformations must exist which can crystallize together with the syndiotactic chain segments in the orthorhombic lattice described by Natta and Corradini.

There is some additional experimental evidence for the importance of straight chain conformations in polymers. Measurements of the density of polymer materials show that the difference in density between the 100% crystalline and 100% amorphous forms of a polymer is often small. For PVC Lebedev *et al.*[30] found a density of 1.44 g/cm^3 for the crystalline phase and 1.41 g/cm^3 for the amorphous phase.

Robertson[64], who observed similar small differences between the densities of the crystalline and amorphous phases of many polymers, argues that even in the amorphous phase the polymer chains should be more or less straight and aligned in parallel. This is the second reason why particular attention must be given to straight chain conformations.

Construction with gauche pairs gives bulky chains or comparitively wide helices. Moreover, such chain conformations do not resemble the all-trans syndiotactic chain, thus making co-crystallization impossible. However, combination of trans pairs results in straight chains or slender helices. The following part of this chapter contains the results of our studies on these straight chain conformations of PVC.

The syndiotactic parts of the chain pose no problem. All literature reports indicate that these segments assume the very regular all-trans conformation. The same was found with the atomic models. The zig-zag conformation has no steric hindrance and, therefore, has a low chain energy. The conformation is:

---(TR)T(TL)T(TR)T(TL)T(TR)--- *etc.*

Natta and Corradini conclude that crystallites are essentially built up from the above chain segments.

For the isotactic parts of the chain two possible conformations were found in the present work. The first one is the well-known helix conformation. This chain conformation has no steric hindrance; consequently, the chain energy is low. The conformation is as follows:

---(TR)G_l(TR)G_l(TR)G_l(TR)G_l(TR)--- *etc.* or the mirror image:

---(TL)G_r(TL)G_r(TL)G_r(TL)G_r(TL)--- *etc.*

The second possible isotactic conformation is a straight chain composed of two different pair conformations. One of these, $(TR)G_{l}(TR)$, is the same as was used for the helix conformation. The other, $(TR)G_{r}(TR)$, has some steric hindrance; as a consequence, the chain energy of the isotactic straight chain is higher than that of the isotactic helix. This straight chain conformation is represented by:

$---(TR)G_{l}(TR)G_{r}(TR)G_{l}(TR)G_{r}(TR)---$ *etc.* or the mirror image:

$---(TL)G_{r}(TL)G_{l}(TL)G_{r}(TL)G_{l}(TL)---$ *etc.*

Figure 5.3. shows photographs of the three chains. The pictures indicate that the syndiotactic chain and the isotactic straight chain

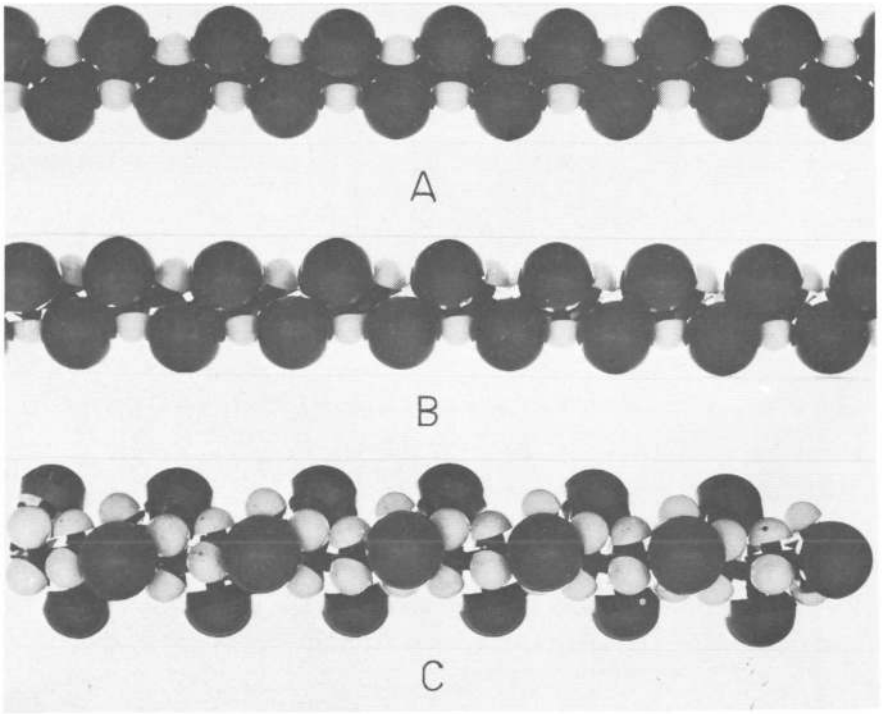

Figure 5.3. Photographs of three different chain conformations.

A syndiotactic straight chain

B isotactic straight chain

C isotactic helix

closely resemble each other. The chlorine-to-chlorine distance along the chain is almost the same in these two cases (5.1 A for the syndiotactic, 5.0 A for the isotactic chain), which is very important for the formation of crystalline structures. A second advantage of the isotactic straight chain over the isotactic helix is the better spatial filling of the former: a closer molecular packing of syndiotactic and such straight isotactic parts of the chains is possible[2].

The disadvantage of the proposed isotactic chain conformation is its higher chain energy because a pair with some steric hindrance is used in constructing it. To establish whether the chain energy is sufficiently low for the isotactic straight chain to be a probable structure, its chain energy has been calculated and compared with the energy of the isotactic helix. This is reported in the next section.

5.4. Calculation of chain energy

The internal energy of a polymer material is composed of two parts: intermolecular and intramolecular energy.

The intermolecular energy depends on the packing and alignment of the chains. No attempt was made to calculate this intermolecular energy. However, one can make this qualitative statement: when straight chains are closely packed the intermolecular energy decreases. In fact, this is the very reason why crystallization occurs. Thus it can be concluded that -from an intermolecular point of view- straight chain conformations are energetically favourable.

The intramolecular energy of the chain is determined by its conformation. Since this conformation can be described (see above) it is now possible to calculate the intramolecular energy. The calculations were performed according to a method used for PVC by Fordham[24] which was improved later on by Glazkovskii and Papulov[65]. In this method the contribution to the intramolecular energy is divided into the electrostatic energy and the steric energy. The steric energy is the sum of all Van der Waals attractions and repulsions of atoms not joined by valence bonds. The electrostatic energy was calculated from the dipole-dipole interaction of the CCl-dipoles.

The calculation requires the knowledge of all interatomic distances. To this end, the spatial arrangement has to be translated into a coordination scheme of all the atoms of the chain segment under consideration. For the calculation of the chain energies of the three important conformations one must know the energies of three pairs, *viz.* the syndiotactic pair conformation (TR)T(TL) and the isotactic pair conformations, (TR)G_l(TR) and (TR)G_r(TR). The syndiotactic straight chain is a combination of the pairs (TR)T(TL) and (TL)T(TR) which both have the same energy. The isotactic helix is composed of the (TR)G_l(TR) *or* (TL)G_r(TL) pairs; again, these pairs have the same energy. The isotactic straight chain consists of the (TR)G_l(TR) *and* (TR)G_r(TR) pairs (or their mirror images). These pairs have different energies and the chain energy is the average of the two pair energies.

The calculation of the pair energy proceeds as follows:

1. Coordinate axes are chosen and the coordinates of the two chlorine atoms, four carbon atoms and six hydrogen atoms are established.
2. All interatomic distances are calculated.
3. The dipole-dipole interaction is determined.
4. The steric energy is calculated.
5. The total intramolecular energy is obtained by summation of the electrostatic and the steric energy.
6. In one case rotation around a C-C bond is introduced to eliminate high steric hindrance. The calculation is then repeated until the minimum pair energy is found.

5.4.1. Coordinate system

Rectangular space coordinates were used. However, in the PVC chain all bond angles are equal to the valence bond of tetrahedral carbon ($\phi = 109^{\circ}29'$). Especially when rotations in the carbon skeleton are introduced 'tetrahedral axes' are useful since the coordinates then are very simple and the rotations around C-C bonds are easily described.

The distances between the atoms are calculated with the aid of the

cosine rule. If coordinates X, Y and Z of two atoms differ by ΔX, ΔY and ΔZ, respectively, the distance between them is found from:

$$d^2 = \Delta X^2 + \Delta Y^2 + \Delta Z^2 + 2\cos\phi(\Delta X\Delta Y + \Delta X\Delta Z + \Delta Y\Delta Z) \qquad (5.1)$$

With rectangular axes $\cos\phi = 0$, for the tetrahedral coordinates $\cos\phi = -\frac{1}{3}$.

5.4.2. Electrostatic energy

The electrostatic energy is calculated from dipole-dipole interaction. The dipole moment of ethylchloride (2.05 D) is assumed to be concentrated in the C-Cl dipole. Since all interatomic distances are known (see previous section) it is convenient to perform the calculation of the electrostatic factor with a Coulomb-type equation. The dipole moment μ originates from two electric charges (+ q) and (- q) located in the carbon and chlorine nuclei, respectively. With the known values of μ and d_{CCl} we calculate:

$$q = \frac{\mu}{d_{CCl}} = \frac{2.05}{1.76}\ \text{D/A}$$

$$= 1.16 \times 10^{-10}\ \text{e.s.u.} \qquad (5.2)$$

The electrostatic energy is then determined with the equation

$$E_{el} = q^2\left(\frac{1}{r_{CC}} + \frac{1}{r_{ClCl}} - \frac{1}{r_{CCl_1}} - \frac{1}{r_{CCl_2}}\right) \qquad (5.3)$$

where

q = electric charge

r_{CC} = distance between the two carbon nuclei of the interacting CCl-dipoles

r_{ClCl} = distance between the two chlorine nuclei and

r_{CCl_1} and r_{CCl_2} = distance between carbon atom and chlorine atom not connected to each other by a valence bond.

When the factor q^2 is expressed in kcal. A/mole units, its value is 19.5.

5.4.3. Steric energy

A set of equations assembled by Glazkovskii and Papulov[65] was applied for the calculation of the steric energy. They used Van der Waals potentials published by Hill[66], Crowell[67], and Meeson and Kreevoy[68,69] for the interaction of non-bonded atoms. The potentials were measured with inert gases having almost the same atomic size as the hydrogen, carbon and chlorine atoms, *viz.* helium, argon and krypton, respectively. The interaction potentials all have the form:

$$E_{st} = K\, e^{-ar} - K' r^{-6} \qquad (5.4)$$

Where

E_{st} = steric energy (kcal/mole)

r = distance between the two nuclei

a,K,K' = constants (see table 5.2.).

Table 5.2. Constants in the interaction potential equation (5.4)

Interacting atoms	$K \times 10^{-3}$ kcal/mole	K' kcal·A^6/mole	a A^{-1}	Reference
H...H	35	18	5.7	Hill[66]
C...C	40	350	3.6	Crowell[67]
Cl...Cl	220.8	1430	3.621	Meeson and Kreevoy[68,69]
C...H	37.4	79	4.65	*
C...Cl	94	707	3.6	*
H...Cl	88	161	4.65	*

* The constants for the potentials between different atoms were calculated on the basis of the combination rule[65].

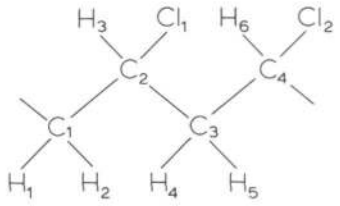

Figure 5.4. Numbering of the atoms within a pair.

Table 5.3. Survey of the atomic interactions in a pair of monomer units.

Interacting atoms	H...H	C...C	Cl...Cl	C...H	C...Cl	H...Cl
	$H_1...H_3$ $H_1...H_4$ $H_1...H_5$ $H_1...H_6$ $H_2...H_3$ $H_2...H_4$ $H_2...H_5$ $H_2...H_6$ $H_3...H_4$ $H_3...H_5$ $H_3...H_6$ $H_4...H_6$ $H_5...H_6$	$C_1...C_4$	$Cl_1...Cl_2$	$C_1...H_4$ $C_1...H_5$ $C_1...H_6$ $C_2...H_6$ $C_3...H_1$ $C_3...H_2$ $C_4...H_1$ $C_4...H_2$ $C_4...H_3$	$C_1...Cl_2$ $C_2...Cl_2$ $C_4...Cl_1$	$H_1...Cl_1$ $H_1...Cl_2$ $H_2...Cl_1$ $H_2...Cl_2$ $H_3...Cl_2$ $H_4...Cl_1$ $H_4...Cl_2$ $H_5...Cl_1$ $H_5...Cl_2$ $H_6...Cl_1$

Figure 5.4. shows a chain segment consisting of two monomer units. The atoms of this pair are numbered C_1 until C_4, H_1 until H_6, Cl_1 and Cl_2. The total steric energy of this pair is found by summation of the potentials of 37 interactions, listed in table 5.3. Only the interactions that depend on the conformation are taken into consideration. For example, the distance between the atoms C_1 and C_3 does not change upon rotation around a carbon-to-carbon bond and, consequently, the C_1---C_3 potential is constant. However, the distance between the atoms H_1 and H_3 changes upon rotation around the C_1---C_2 bond. Therefore, this H_1---H_3 interaction depends on conformation.

5.5. Energies

5.5.1. Pair energies

As we have seen previously three pairs play a role in the occurrence of straight chain conformations. These pairs are:

(TR)T(TL) or (TL)T(TR) , syndiotactic

(TR)G_l(TR) or (TL)G_r(TL), isotactic and

(TR)G_r(TR) or (TL)G_l(TL), isotactic.

The energies of above pairs were calculated with the aid of an IBM 360/65 computer. The results are listed in table 5.4.

Table 5.4. shows a high energy for pair (TR)G_r(TR). According to this result, the conformation of the straight isotactic chain would seem to be unfavourable since this chain conformation contains the

Table 5.4. Energies of pairs of monomer units.
(All energies in kcal/mole)

Pair	E_{el}	ΣE_{st}	E_{tot}
(TR)T(TL)	0.12	- 0.68	- 0.56
(TR)G_l(TR)	0.78	- 1.01	- 0.23
(TR)G_r(TR)	0.12	32.25	32.37

high energy pair. The detailed information from the computer showed that the high energy for pair (TR)G_{γ}(TR) is caused by the steric hindrance between one of the hydrogen atoms and one of the chlorine atoms, *viz.* H_1---Cl_2. This was confirmed by the Courteauld Atomic Models. However, it was also found that a clockwise rotation around the C-C bond of the second monomer unit causes the steric energy to fall off rapidly. This rotation was introduced in the pair (TR)G_{γ}(TR) and its energy was recalculated in the following manner.

When deviations from the staggered position occur the potential energy due to internal rotation must be taken into account. This potential energy is estimated by a function[70,71]

$$E_{rot} = \frac{E_o}{2} (1 - \cos 3\gamma) \qquad (5.5)$$

where E_o = potential barrier, kcal/mole and
γ = deviation from the staggered position.

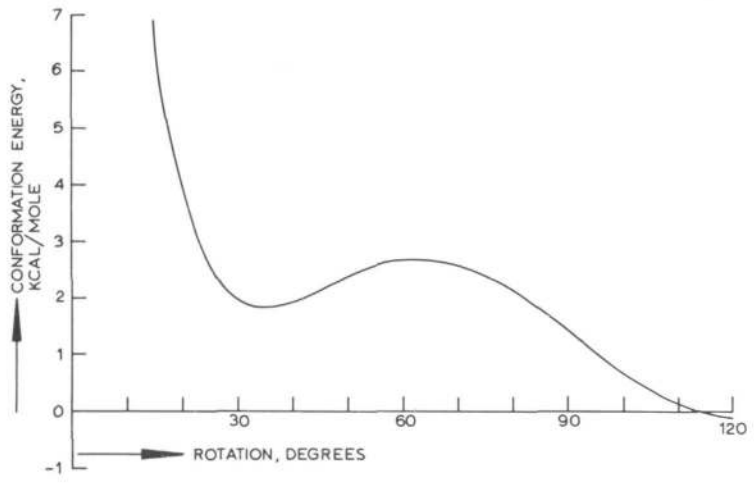

Figure 5.5. Conformation energy of pair (TR)G_{γ}(TR) as a function of the angle of rotation (explanation: see text).

Using the value E_o = 3 kcal/mole (potential barrier of ethane[72]) the conformational energy is calculated with the equation

$$E_{tot} = E_{rot} + E_{el} + \Sigma E_{st} \qquad (5.6)$$

Figure 5.5. shows that a minimum energy of the pair (TR)G_p(TR) of about 1.8 kcal/mole is obtained by a rotation over 35°.

The pair energies revised in this way are listed in table 5.5.

Table 5.5. Energies of pairs of monomer units (revised)
(All energies in kcal/mole)

Pair	E_{el}	ΣE_{st}	E_{rot}	E_{tot}
(TR)T(TL)	0.12	- 0.68	0	- 0.56
(TR)G_l(TR)	0.78	- 1.01	0	- 0.23
(TR)G_p(TR)	0.16	0.15	1.5	1.8

5.5.2. Chain energies

Ultimately we are interested in the energies of the two straight chain conformations, syndiotactic and isotactic, and that of the isotactic helix. To calculate these chain energies from the pair energies certain restrictions have to be made. The segment in figure 5.6. contains two pairs, one with the carbon atoms C_1-C_2-C_3-C_4 and one with the atoms C_3-C_4-C_5-C_6.

When calculating the energy of this segment by simply averageing the pair energies three errors are made:

1. Steric interactions within the monomers are counted twice. A correction must be made because interactions H_4---H_6, H_4---Cl_2, H_5---H_6, H_5---Cl_2 are part of the first as well as the second pair (correction 1 in table 5.6.).

2. Steric interactions over long distances are neglected. The most important of these is the interaction $C_2 \cdots C_5$. However, in the straight chain conformations considered here the error is quite small (correction 2 in table 5.6.).

Table 5.6. Chain energies
(All energy contributions in kcal/mole)

Chain conformation	Pair conformations	Pair energies	Average value
syndiotactic, straight chain	(TR)T(TL) (TL)T(TR)	- 0.56 - 0.56	- 0.56
isotactic, helix	(TR)G_l(TR) (TR)G_l(TR)	- 0.23 - 0.23	- 0.23
isotactic, straight chain	(TR)G_l(TR) (TR)G_p(TR)	- 0.23 1.8	0.8

Chain conformation	Average value	corrections			chain energy
		1	2	3	
syndiotactic, straight chain	- 0.56	0.28	- 0.1	0.40	0
isotactic, helix	- 0.23	0.28	- 0.1	0.40	0.3
isotactic, straight chain	0.8	0.25	- 0.1	0.35	1.3

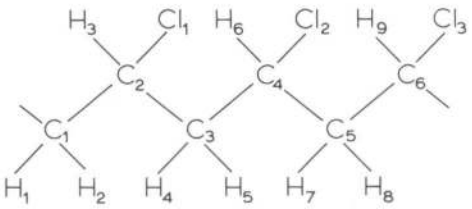

Figure 5.6. Chain segment consisting of two overlapping pairs.

3. Dipole interactions over long distances are neglected too, e.g. the interaction between dipoles C_2---Cl_1 and C_6---Cl_3. The electrostatic energies are calculated in order to compensate for this effect. It is found that the corrections have almost the same value for the three chain conformations (correction 3 in table 5.6.).

Table 5.6. summarizes the final results of the calculation of the chain energies after correction for the three sources of error. The difference in the chain energies of the isotactic helix and the isotactic straight chain is but small (1.0 kcal/mole). Therefore it is very likely that -below the glass transition temperature- a large fraction of the isotactic material has assumed the straight chain conformation.

The chain structure can be investigated experimentally by nuclear magnetic resonance and infrared measurements. A survey of the literature reports on this subject is given below. It is of interest to learn from these experimental results whether the isotactic straight chain conformation indeed exists and to what extent it occurs in PVC.

5.6. Chain structure analysis

5.6.1. NMR analysis

The chain conformation can be studied on the basis of the observed coupling constants between the methylene and the methine protons. With

liquid model compounds like the stereoisomers of 2,4-dichloropentane (DCP)[3,7] and 2,4,6-trichloroheptane (TCH)[3,6] it was found that the trans conformation is the stable form of the syndiotactic compounds of DCP and TCH whereas the isotactic compounds have the helix conformation.

These results indicate that the stable, low-energy conformation will be all-trans or helix-like for syndiotactic and isotactic PVC, respectively. This applies to PVC in solution. However, as was mentioned in the previous section, other conformations may also occur in the bulk. Unfortunately, the conformation of the chains in solid PVC samples cannot be studied with NMR because solid samples give broad spectral bands from which no information about the chain structure can be derived.

5.6.2. IR analysis

5.6.2.1. CCl-stretching vibrations

Almost all the literature reports in which information is given on the chain structure deal with the region in the infrared spectrum where the carbon-to-chlorine stretching vibrations absorb. This part of the spectrum is shown in figure 5.7. which was taken from the work of Krimm[73]. The spectrum consists of three bands located at 615, 635 and 690 cm^{-1}, respectively. The bands at 615 and 635 cm^{-1} strongly overlap. Moreover, the three bands are all complex since each band consists of at least two different absorption frequencies.

The absorption frequency depends on the spatial arrangement of the atoms around the carbon-to-chlorine bond. With the aid of the information from the spectra of low molecular weight model compounds it is possible to assign the absorption bands to different 'local' conformations around the CCl-bond. These local arrangements occur in different chain conformations and, hence, the spectrum can be interpreted in terms of chain conformations. Therefore, a qualitative impression can be obtained concerning the occurrence of the various chain conformations in bulk PVC.

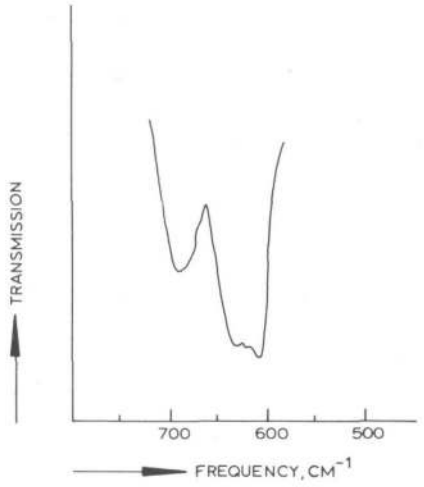

Figure 5.7. Infrared spectrum of PVC obtained by polymerization at 50°C, KBr pellet (According to Krimm[73]).

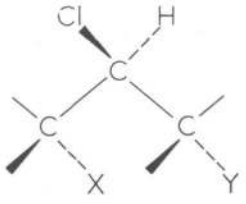

Figure 5.8. Nomenclature of CCl-stretching vibrations.

5.6.2.2. Nomenclature

The nomenclature of the frequencies of the CCl-stretching vibrations is based on the geometrical arrangement around the CCl-bond. The symbol S is used because the chlorine atom is attached to a secondary carbon atom, and two subscripts are added for the two atoms in trans position relative to the chlorine atom.

Figure 5.8. shows the conformation of the chain in the neighbourhood of one chlorine atom. The two trans substituents are X and Y, respectively; hence, the IR absorption of this conformation is called S_{XY}.

The substituents X and Y can be carbon or hydrogen. When the carbon backbone is planar there are two hydrogen atoms in trans position and the conformation is then indicated by S_{HH}. There is another conformation in which two hydrogen atoms are in trans position but here the carbon chain is not planar. This conformation is indicated by $S_{HH'}$. Thirdly, an arrangement exists with one carbon and one hydrogen atom in the trans position, S_{CH}. These three conformations are shown in figure 5.9. On paper it is possible to construct three additional arrangements -$S_{H'H'}$, S_{CC} and $S_{CH'}$- which occur in some low molecular weight compounds (e.g. chlorocyclohexane)[73], but they do not exist in PVC because of steric hindrance.

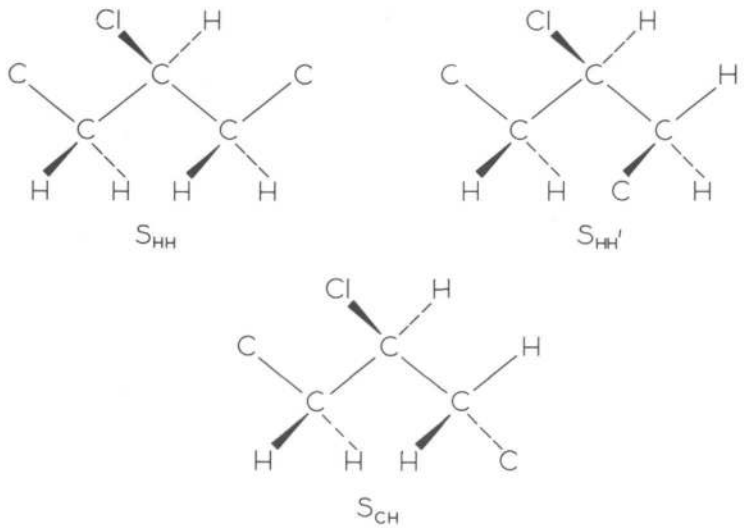

Figure 5.9. Conformations of the PVC chain. Nomenclature of the CCl-stretching vibrations.

5.6.2.3. Main absorption frequencies

Secondary alkyl chlorides have been examined as model compounds for PVC. The IR absorption frequencies of these compounds are collected in table 5.7.

Table 5.7. Absorption frequencies of model compounds

Conformation	Absorption frequency, cm^{-1}	Examples
S_{HH}	611	2-chloropropane
$S_{HH'}$	627-637	2-chlorobutane[75]
		2,3-dichloropentane[73,76,77]
		2,4,6-trichloroheptane[73,76]
S_{CH}	667	2,2-dimethyl-3-chlorobutane[74]

The arrangements S_{HH}, $S_{HH'}$, ans S_{CH} are also found in the PVC chain conformations. S_{HH} occurs in the syndiotactic straight chain conformation and the isotactic helix contains S_{CH} arrangements only. The isotactic straight chain consists of alternating S_{CH} and $S_{HH'}$ arrangements. The S_{CH} arrangement is also found in syndiotactic chain segments with a helix conformation. This conformation occurs to some extent in bulk PVC but the helix conformations are not important in connection with the chain structure in crystalline material. Therefore, no attention is given to the S_{CH} absorption.

It is possible to summarize the infrared band assignment as follows:

1. the S_{HH} absorption at 615 cm^{-1} originates from syndiotactic straight chain segments.
2. the $S_{HH'}$ absorption at 635 cm^{-1} is assigned to isotactic straight chain segments.
3. the S_{CH} absorption at 690 cm^{-1} originates from the isotactic straight chains as well as from isotactic and syndiotactic helix conformations.

5.6.2.4. Additional absorption frequencies

In the infrared spectrum of PVC two absorption frequencies are found which are absent in the spectra of the low molecular model compounds. For example, urea complex-produced PVC which has a very high degree

of syndiotacticity, gives a spectrum in which only absorptions at 603 and 640 cm^{-1} are found.

One would expect that such a syndiotactic material would give strong absorption at 615 cm^{-1}. The absence of this absorption is explained by the coupling of CCl-stretching vibrations in long syndiotactic zig-zag chain segments which results in a split up of the S_{HH} band at 615 cm^{-1} into the bands at 603 and 640 cm^{-1} [21,22,74,78,79]. Pohl and Hummel[21] calculated that this coupling requires a minimum length of the syndiotactic zig-zag chain segments of five monomer units. These rather short sequences are present even in atactic PVC and, therefore, it is not surprising that these absorptions at 603 and 640 cm^{-1} are also found in the spectrum of atactic PVC. They cause a lot of trouble in the interpretation of the spectrum: the band at 603 cm^{-1} shows up as a shoulder on the S_{HH} absorption band at 615 cm^{-1} and the 640 cm^{-1} absorption almost coincides with the $S_{HH'}$ absorption at about 635 cm^{-1}.

Table 5.8. Assignment of absorption bands

Frequency, cm^{-1}	Tacticity	Conformation	Chain conformation
603	s	S_{HH}	syndiotactic straight chain, long segments
615	s	S_{HH}	syndiotactic straight chain, short segments
635	i	$S_{HH'}$	isotactic straight chain
640	s	S_{HH}	syndiotactic straight chain, long segments
690	i and s	S_{CH}	isotactic straight chain, isotactic helix and syndiotactic helix

5.6.2.5. Assignment of absorption frequencies

Many authors have reported on the assignment of the absorption bands[21,22,80,81,82,83,84,85]. Krimm's survey[78] and recent publications by Hummel and Pohl[22] and Glaskovskii *et al.*[84] have been used to assemble table 5.8. in which the band assignment is given.

5.6.2.6. The isotactic straight chain conformation

The absorbance at 635 cm^{-1} is a measure of the fraction of polymer with the isotactic straight chain conformation. A quantitative evaluation is not possible because the bands at 635 and 640 cm^{-1} strongly overlap[21,22] but a qualitative approach can be made. The absorption bands at 615 and 635 cm^{-1} have almost the same size. The first band is a combination of syndiotactic S_{HH} absorption and the syndiotactic component at 603 cm^{-1}, the second one consists of the isotactic S_{HH}, absorption and the syndiotactic band at 640 cm^{-1}. The spectrum of urea complex-produced PVC reveals that the syndiotactic contributions at 603 and 640 cm^{-1} are equally large and therefore we conclude that the isotactic 635 cm^{-1} absorbance is of the same order of magnitude as the syndiotactic S_{HH} absorbance at 615 cm^{-1}. This implies that a large fraction of the isotactic chain segments has the straight chain conformation.

Opaskar[76] calculated the normal vibrations of the isotactic helix conformation and his results show that long chain segments with this conformation are not present in bulk material. The same conclusion was drawn by Koenig *et al.*[86] from the results of Raman and IR spectra. This supports the above conclusion that the isotactic material is not present as helices.

Summarizing, the discussion presented in the present chapter shows that

1. the isotactic straight chain has a chain energy which is only slightly higher than that of the isotactic helix.

2. the infrared absorbance from the isotactic straight chain segments is of the same order of magnitude as the absorbance from the syndiotactic straight chain segments.
3. the isotactic helices are not present in bulk PVC.

All these facts lead to the conclusion that isotactic straight chains occur in bulk PVC in appreciable quantities.

5.7. Conclusions

1. The syndiotactic chain with the lowest energy has the planar zig-zag conformation
   --(TR)T(TL)T(TR)T(TL)-- *etc.*
2. The isotactic chain conformation with the lowest energy is the isotactic helix
   --(TR)G_l(TR)G_l(TR)G_l(TR)-- *etc.*
3. There exists an isotactic chain conformation with a slightly higher energy. This is a straight chain which very closely resembles the syndiotactic straight chain; its conformation is:
   --(TR)G_l(TR)G_r(TR)G_l(TR)G_r(TR)-- *etc.*
4. Infrared analysis of the chain structure shows that a large fraction of the isotactic chain segments has the straight chain conformation.

CHAPTER 6

CRYSTALLINE STRUCTURE

6.1. Introduction

Although both syndiotactic and atactic PVC can crystallize, the syndiotactic materials crystallize more readily than atactic PVC because the molecular packing is energetically more favourable with pure syndiotactic zig-zag chains. This conclusion is supported by literature data: high crystalline contents are only found in highly syndiotactic polymerizates.

A special case are the PVC's obtained by polymerizing in the presence of butyraldehyde which exhibit a high degree of syndiotacticity combined with a low molecular weight. Similarly, high crystallinity occurs with PVC obtained by irradiating the urea inclusion complex of vinyl chloride at $-78^{\circ}C$[87]. The resulting polymers are very highly tactic and therefore equally highly crystalline.

With commercially important polymerization techniques like emulsion and suspension processes, the polymerization temperature is the most important factor influencing the tacticity of the polymer. At temperatures below $0^{\circ}C$ partly syndiotactic PVC is obtained and such low temperature polymerizates are crystalline. However, crystallinity is not determined solely by the tacticity but also by the mechanical and thermal history of the PVC. Stretching of PVC fibres, for instance, raises the crystallinity of the material. Less severe mechanical handling like calendering and extrusion also influences the crystalline structure[88,89]. The effects of the thermal history of PVC on its crystallinity were described in chapter 3.

Crystallinity can be observed by electron microscopy and by means of X-ray diffraction. With special care it is possible to create single crystals of PVC. Electron microscopy and X-ray measurements have both been applied to such single crystals. However, the crystallites in PVC are usually too small for electron microscopy, especially when

crystallization occurs in the bulk. Measurement of X-ray diffraction then is the only suitable means of studying the crystalline structure. A sufficient number of literature reports are available on this subject for an understanding of the crystal forms of PVC. This literature will be reviewed.

6.2. Single crystals

The most convincing evidence of the existence of crystallinity is that single crystals of PVC can be prepared. Smith and Wilkes[90] obtained them from 2% chlorobenzene solutions of highly syndiotactic, low molecular weight PVC polymerized in the presence of butyraldehyde. Their crystals were rectangular in shape and approximately 100 A thick which represents the length of the extended chains. The X-ray diffraction diagram showed that the crystals were orthorhombic.

Nakajima and Hayashi[91] produced single crystals from syndiotactic as well as atactic PVC. All their polymers had a high molecular weight. Invariably, single crystals were obtained by slowly cooling 0.1% chlorobenzene solutions. The atactic commercial PVC gave strip-shaped crystals with lamellar thickness of 50 - 100 A. This implies that the chains are folded in the crystal and that isotactic chain segments cooperate in forming these crystals since syndiotactic sequences of 20 - 40 monomer units are not present in a commercial PVC (*cf* chapter 2).

6.3. X-ray analysis

Natta and Corradini[29] performed X-ray measurements with oriented fibres of commercial atactic PVC (this work was mentioned earlier in section 5.3.3.). The reflections found by them are indicative of an orthorhombic crystal lattice with axes a = 10.6 A, b = 5.4 A and c = 5.1 A. Figure 6.1. shows the ab-plane of this lattice. Results of X-ray measurements on single crystals of PVC strongly support the conclusions of Natta and Corradini: the single crystals show the same orthorhombic X-ray diffraction pattern as the crystallites formed from bulk polymer[90,91].

In X-ray diagrams of PVC (especially atactic PVC) sometimes a

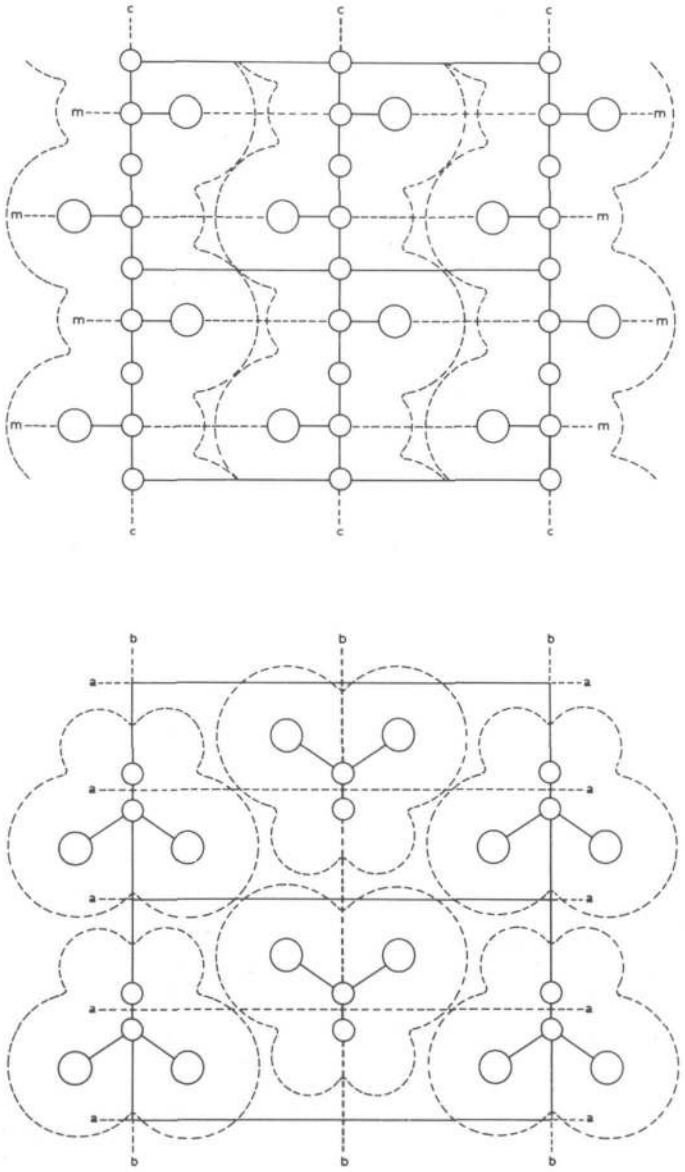

Figure 6.1. Model of the orthorhombic structure of polyvinyl chloride (According to Natta and Corradini[29]).

diffraction ring is found which cannot be ascribed to the orthorhombic crystal form. Mammi and Nardi[92,93] describe this reflection as being due to mesomorphic or nematic structures which appear after annealing at 85 - 107°C of stretched fibres. These nematic structures consist of straight chains aligned in parallel with a distance between the axes of 5.4 A.

Lebedev *et al.*[94] report the reflection from 'polymer molecules in parallel arrays, which can be further perfected by concordant rotations, displacements, inclinations, etc.'. In this work the nematic structures are also found after annealing at a temperature above the glass transition region. Another paper of Lebedev[30] shows that annealing at 110°C produces reflections from orthorhombic and nematic structures at the same time, which means that the alignment of chains proceeds simultaneously with the formation of real orthorhombic crystallites.

6.4. Crystallinity of atactic PVC

6.4.1. The orthorhombic lattice

An important conclusion from the literature review in the previous paragraphs is that the orthorhombic crystal form is independent of the tacticity of the PVC: Natta and Corradini[29] performed their measurements with atactic PVC, Smith and Wilkes[90] used syndiotactic 'butyraldehyde-PVC' and Nakajima and Hayashi[91] worked with syndiotactic as well as atactic PVC, but they all found the same orthorhombic lattice.

Again, the conclusion must be drawn that the crystalline phenomena in PVC cannot be explained by assuming that only the syndiotactic chain segments crystallize. Consequently, the isotactic chain segments must be able to crystallize. One of the objects of the present study is to elucidate how the isotactic chain segments co-crystallize with syndiotactic chain segments. This is discussed below.

Natta and Corradini[29] assume that the orthorhombic crystals consist of syndiotactic straight chain segments. Their presentation of the orthorhombic lattice (*cf* figure 6.1.) shows this conformation. Our supposition that the isotactic straight chain segments co-crystallize

has to be proved by comparison of the cross-sections and longitudinal sections of the straight chains. For the co-crystallization to be possible there must be a very close resemblance between the syndiotactic and isotactic straight chains since only very small chain deformations are allowed in the orthorhombic crystal lattice.

A comparison of the syndiotactic straight chain with conformation --(TR)T(TL)T(TR)T(TL)--, and the isotactic straight chain having the conformation --(TR)G_l(TR)G_r(TR)G_l(TR)--, is given in the figures 6.2. and 6.3. From the longitudinal sections in figure 6.2. it appears that the chlorine-to-chlorine distance in the direction along the chain is almost the same in the two cases, the syndiotactic chain showing a value of 5.1 A whereas the isotactic value is 5.0 A.

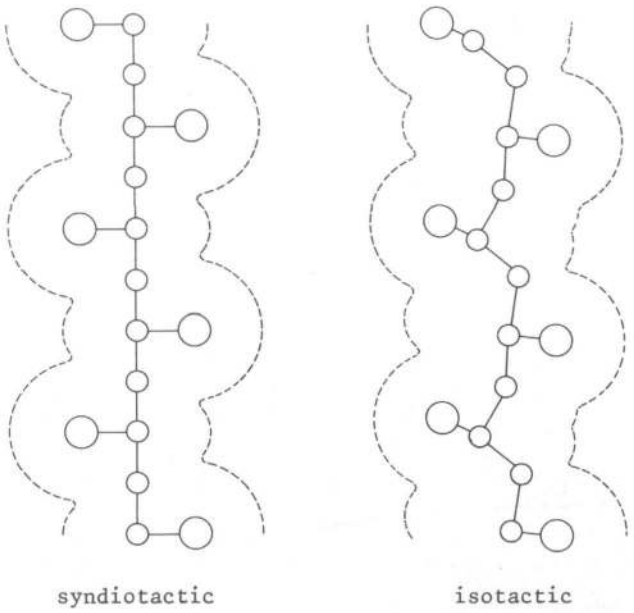

Figure 6.2. Comparison of the syndiotactic and isotactic straight chains. Longitudinal section.

Another small difference is a minor longitudinal shift of the chlorine atoms on the isotactic chain as compared with those on the syndiotactic chain. These differences decrease the regularity along the c-axis of the crystal lattice. This is in line with the statement by Natta and Corradini that there is 'lack of order along the c-axis'.

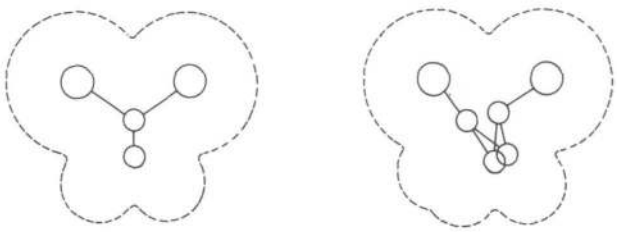

Figure 6.3. Comparison of the syndiotactic and isotactic straight chains. Cross-section.

The cross-sections of the two chains are also almost similar (figure 6.3.) because the chlorine atoms occupy the same positions. The only difference is the width at the position of the methylene groups: there the isotactic chain is somewhat wider. In spite of this, the isotactic chain fits perfectly in the orthorhombic cell together with the syndiotactic chain segments. This is shown in figure 6.4. in which isotactic chains are surrounded by syndiotactic chains.

The above comparison reveals that the co-crystallization of isotactic chain segments with the syndiotactic chains is possible. However, it does not explain the relatively high percentage of crystallinity found in atactic PVC. In the atactic chain there is a random distribution of syndiotactic and isotactic segments (*cf* chapter 2). These segments are short (average length about 4 monomer

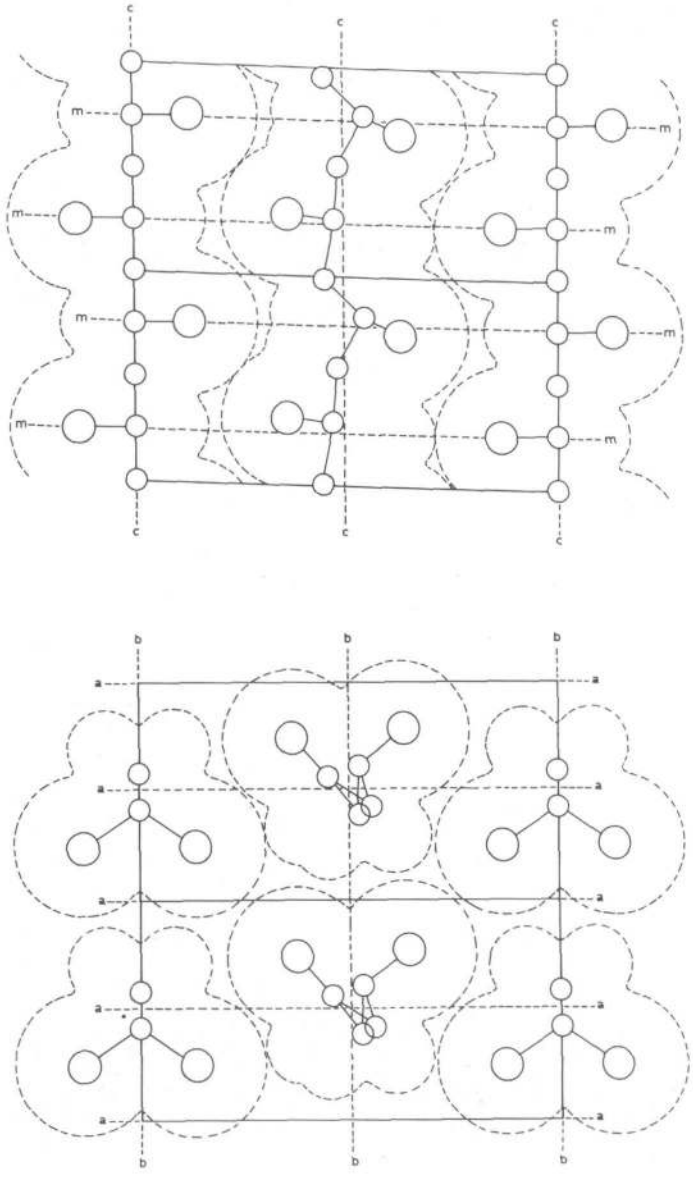

Figure 6.4. Model of the structure of polyvinyl chloride. Combination of syndiotactic and isotactic chain segments in the orthorhombic lattice.

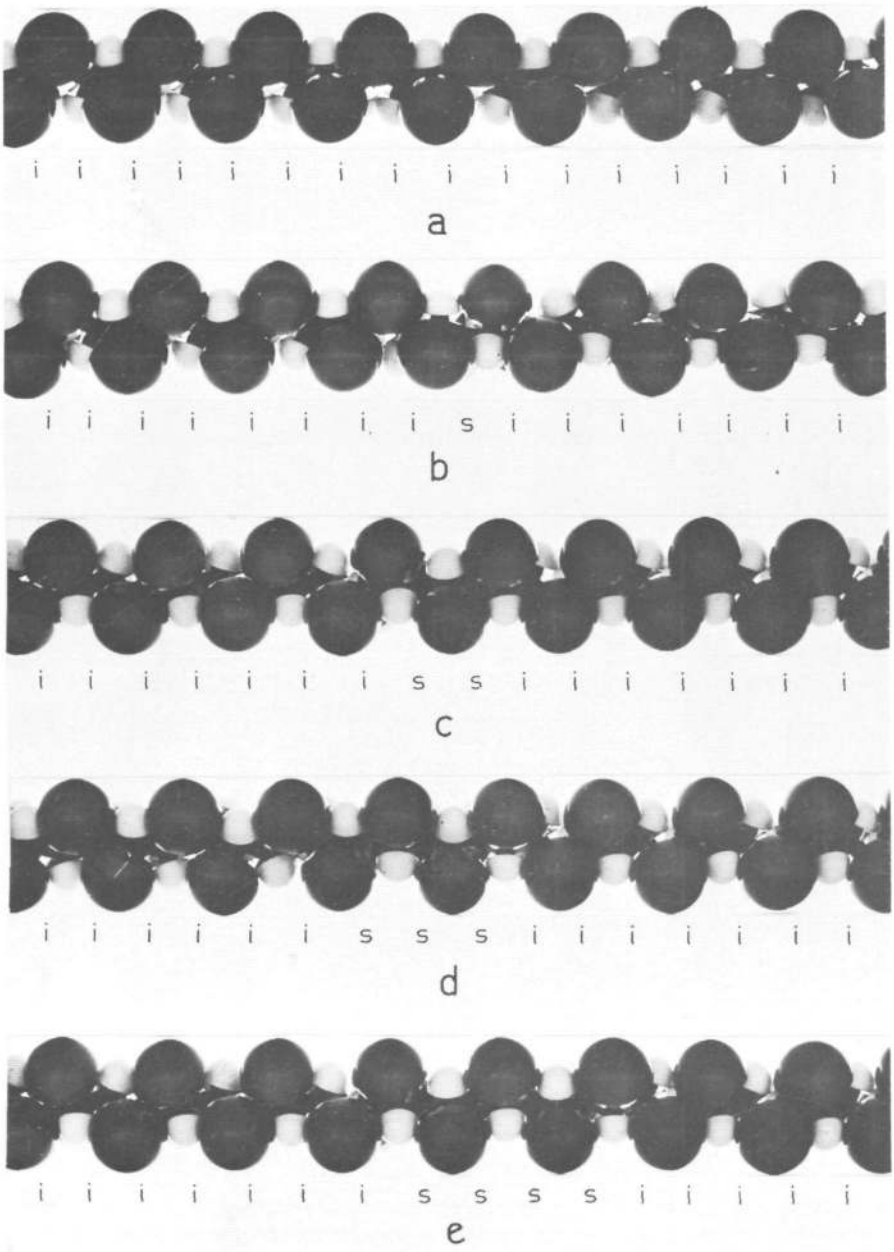

Figure 6.5. Photographs of PVC chains; occurrence of discontinuities.

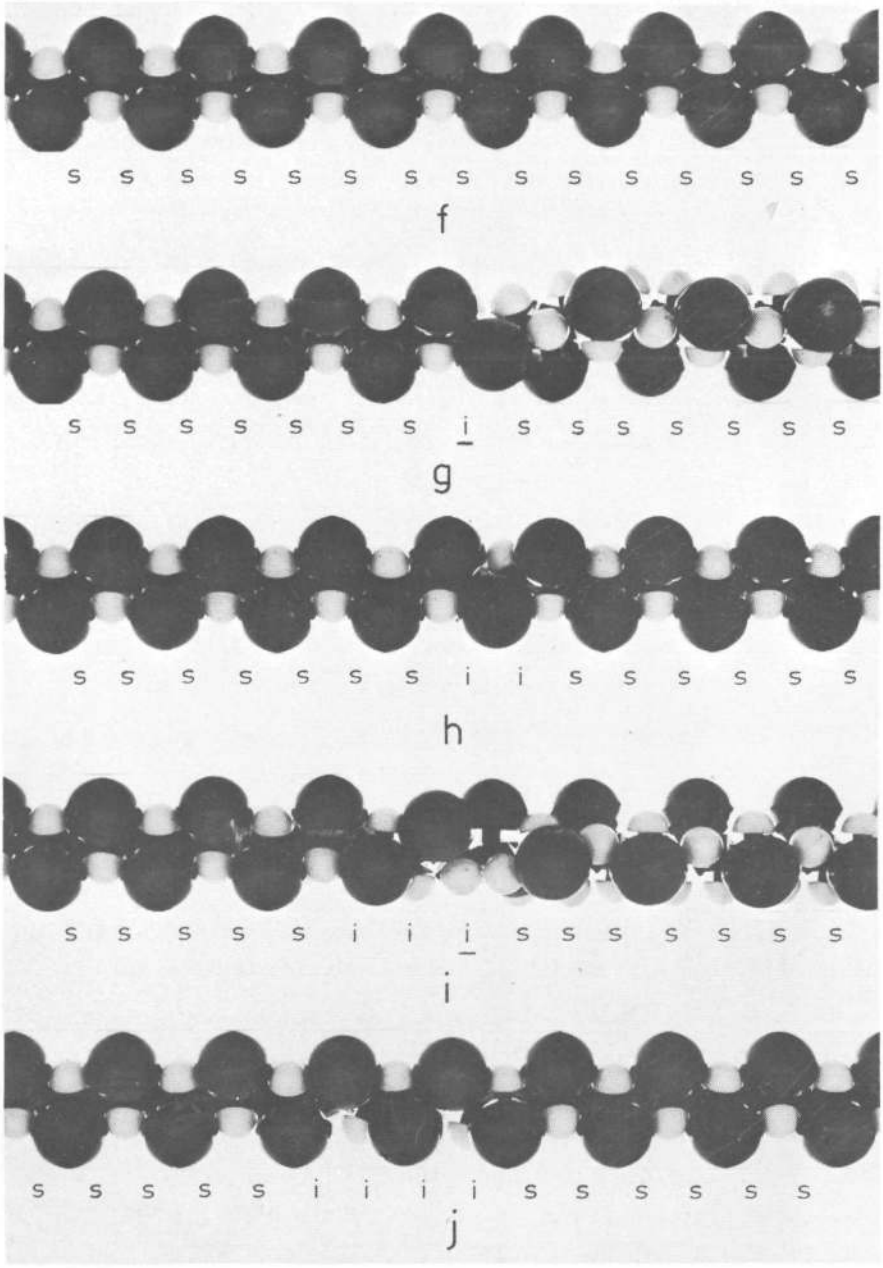
s s s s s s s s s s s s s s s
f
s s s s s s s i s s s s s s s
g
s s s s s s s i i s s s s s s
h
s s s s s i i i s s s s s s s
i
s s s s s i i i i s s s s s s
j

units) and, consequently, there are many transitions between the two types of segments.

The question arises whether these 'tacticity transitions' can be built into the crystal lattice. In order to answer it atactic chains were constructed from atomic models. First, syndiotactic sequences were introduced into a fully isotactic chain and then isotactic sequences into a syndiotactic chain. Figure 6.5. shows photographs of all these chains.

The photographs 6.5. a, b, c, d and e show that the introduction of syndiotactic sequences into an isotactic chain does not disturb the chain structure. The regular succession of chlorine atoms alternately at the sides of the chain is maintained. This is not always the case when isotactic sequences occur in fully syndiotactic chains. Photographs 6.5. g and i show discontinuities: there is a twist in the chain. In figure 6.5. g one isotactic sequence occurs between syndiotactic sequences whereas in figure 6.5. i the number of isotactic sequences is three. In general, a configuration which contains an odd number of isotactic sequences between two syndiotactic sequences causes a discontinuity. In formula, such a configuration is written down as

$$s(i)_{2n+1}s$$

where n = 0, 1, 2, 3 etc.

s = symbol for a syndiotactic sequence of two monomer units

i = symbol for an isotactic sequence of two monomer units.

It is quite impossible that such a discontinuity can be incorporated in the orthorhombic lattice. As a consequence, only the straight atactic chain segments between these chain defects are crystallizable. However, when these straight chain segments crystallize they should have a minimum length according to Flory's theory (*cf* chapter 2).

Below, the distribution of the length of the straight chain segments is calculated and with the resulting distribution a new estimate of the crystallinity in atactic PVC is presented.

6.4.2. Calculation of the crystalline content

We have seen that a discontinuity in the chain arises when an odd number of isotactic sequences is placed between two syndiotactic sequences. When the syndiotacticity α is known the occurrence of these discontinuities as well as the distance between two subsequent discontinuities can be calculated statistically.

The probability of the occurrence of a syndiotactic sequence is α, and hence that of an isotactic sequence is $(1 - \alpha)$, where α is the syndiotacticity of the PVC. One discontinuity is taken as the starting point; the number of sequences between this discontinuity and the next one is counted. The probability p_N of having the next discontinuity at a distance of N sequences should be calculated.

The calculation proceeds as follows. It was shown before that a configuration

s<u>is</u>

is a discontinuity. The straight chain regularity is interrupted at the position in the chain of the isotactic sequence (*cf* figure 6.5. g). When writing down the configuration the interruption of chain regularity is indicated by underlining the symbol i which causes the defect. This chain defect is taken as the 'starting-point discontinuity' in a chain segment and the occurrence of a second discontinuity is then studied. For example a chain segment with two more sequences can have the following configurations:

configurations	probability of occurrence
s<u>is</u> ii	$(1 - \alpha)^2$
s<u>is</u> <u>is</u>	$\alpha(1 - \alpha)$
s<u>is</u> si	$\alpha(1 - \alpha)$
s<u>is</u> ss	α^2

The second configuration in this list contains another discontinuity. In this case the distance between the two discontinuities is one monomer sequence. The probability that such a second discontinuity occurs at a distance of one sequence from the starting-point discontinuity is

$$p_1 = \alpha(1 - \alpha)$$

This example can be extended to three sequences which give the following configurations and probabilities:

configurations	probability of occurrence
sis iii	$(1 - \alpha)^3$
sis iis	$\alpha(1 - \alpha)^2$
sis isi	$\alpha(1 - \alpha)^2$
sis iss	$\alpha^2(1 - \alpha)$
sis sii	$\alpha(1 - \alpha)^2$
sis sis	$\alpha^2(1 - \alpha)$
sis ssi	$\alpha^2(1 - \alpha)$
sis sss	$\alpha 3$

On the third and fourth row of the above table discontinuities are found at a distance of one sequence; the sixth row shows two discontinuities at a distance of two monomer sequences. The probabilities of their occurrence is

$$p_1 = \alpha(1 - \alpha)^2 + \alpha^2(1 - \alpha)$$
$$= \alpha(1 - \alpha), \text{ and}$$

$$p_2 = \alpha^2(1 - \alpha).$$

This way of calculation can be generalized for longer chain segments. A further example is given in table 6.1. where five sequences are considered. In this table also discontinuities are found that are

Table 6.1. Calculation of the probability p_N of the occurrence of two discontinuities at a distance of N sequences

Conformation	Probability			
Number of sequences between two discontinuities				
1 2 3 4 5	p_1	p_2	p_3	p_4
s i s i i i i i	$\alpha(1-\alpha)$			
s i s i i i i s				
s i s i i i s i			$\alpha(1-\alpha)^3$	
s i s i i i s s				
s i s i i s i i				
s i s i i s i s				$\alpha^2(1-\alpha)^3$
s i s i i s s i				
s i s i i s s s				
s i s i s i i i				
s i s i s i i s				
s i s i s i s i				
s i s i s i s s				
s i s i s s i i				
s i s i s s i s				
s i s i s s s i				
s i s i s s s s				
s i s s i i i i				$\alpha^2(1-\alpha)^3$
s i s s i i i s				
s i s s i i s i				
s i s s i i s s				
s i s s i s i i		$\alpha^2(1-\alpha)$		
s i s s i s i s				
s i s s i s s i				
s i s s i s s s				
s i s s s i i i				
s i s s s i i s			$\alpha^3(1-\alpha)$	
s i s s s i s i				
s i s s s i s s				
s i s s s s i i				
s i s s s s i s				$\alpha^4(1-\alpha)$
s i s s s s s s				
Total	$\alpha(1-\alpha)$	$\alpha^2(1-\alpha)$	$\alpha^3(1-\alpha)$ $+\alpha(1-\alpha)^3$	$\alpha^4(1-\alpha)$ $+2\alpha^2(1-\alpha)^3$

caused by three subsequent isotactic sequences between two syndiotactic ones. The probabilities are listed in the columns with headings 'p_2', 'p_3', 'p_4' and 'p_5'.

The formula for the probability p_N was generalized by examining long chain segments. These tables are not shown in this thesis but the final result is presented. The general formula was found to be:

$$p_N = (1 - \alpha)\alpha^N \sum_{i=0}^{i = \frac{N-1}{2}} \frac{(N - 1 - i)!}{(N - 1 - 2i)!\,i!}\left(\frac{1 - \alpha}{\alpha}\right)^{2i} \qquad (6.1)$$

The fraction of the polymer which is present as straight chain segments with a length of N sequences, $F^N_{straight}$, was found from equation 6.1. The distribution of $F^N_{straight}$ is listed in table 6.2. for various values of the tacticity. Figure 6.6. shows $F^N_{straight}$ for $\alpha = 0.55$ together with the distribution of syndiotactic chain segments of length N, F^N_{syndio}, which was taken from figure 2.8.

Flory's theory can be applied to these crystallizable straight chain segments in the same way as was done in chapter 2, section 5. Instead of the fraction F^N_{syndio} the new fraction $F^N_{straight}$ is used. Again, the minimum sequence length ξ_{min} is introduced to derive the maximum possible amount of crystallinity by calculating the fraction of polymer which is present as chain segments larger than or equal to ξ_{min}. Table 6.3. contains the resulting percentages of crystallinity. Figure 6.7. gives the comparison between the maximum possible crystallinity from syndiotactic chain segments only and the similar value for the crystallization of straight atactic chains. In both cases a tacticity value of 0.55 was assumed. With the value $\xi_{min} = 12$ the old theory, assuming crystallizable syndiotactic chains, gives a crystallinity of 0.45% but the new theory evolved in the present work predicts that the crystallization of atactic chains can yield 8.5% crystallinity. The latter

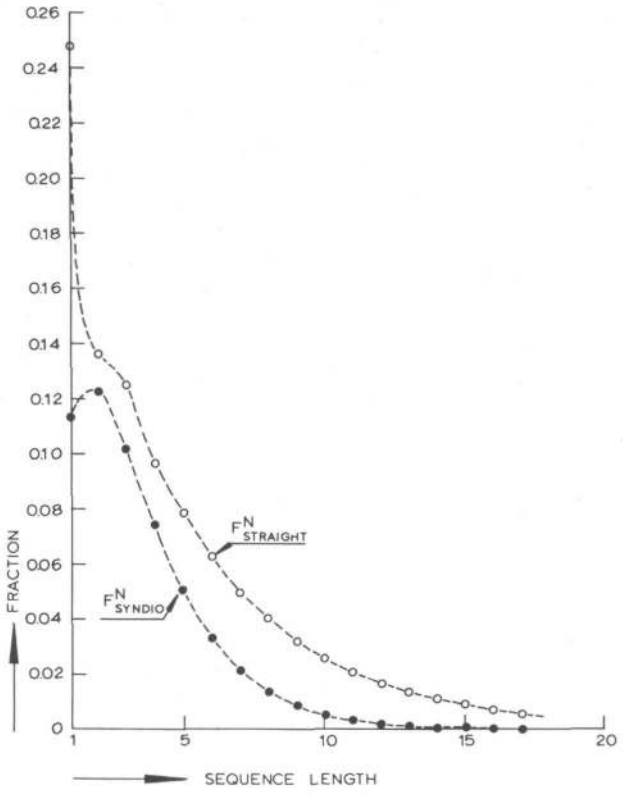

Figure 6.6. Distribution of the sequence length of straight chain segments and syndiotactic chain segments for an atactic PVC with $\alpha = 0.55$.

value is in good agreement with the crystalline contents found in atactic commercial PVC.

However, two restrictions of this theory should be kept in mind:

1. There is less order along the chain axis when the atactic chains crystallize in the orthorhombic lattice as compared with the crystallization of purely syndiotactic chains, and
2. the isotactic straight chain conformation which contributes to the atactic crystallites has a slightly higher energy than the syndiotactic chain.

Table 6.2. Distribution of the length of straight chain segments, $F^N_{straight}$

Number of monomer sequences	tacticity α					
N	0.50	0.55	0.60	0.70	0.80	0.90
1	25.00	24.75	24.00	21.00	16.00	9.00
2	12.50	13.61	14.40	14.70	12.80	8.10
3	12.50	12.50	12.48	12.18	10.88	7.31
4	9.37	9.63	9.79	9.85	9.22	6.72
5	7.81	7.83	7.87	7.99	7.81	6.12
6	6.25	6.26	6.29	6.48	6.62	5.58
7	5.08	4.93	5.03	5.26	5.60	5.08
8	4.10	4.03	4.03	4.26	4.75	4.63
9	3.32	3.23	3.22	3.46	4.02	4.22
10	2.69	2.59	2.58	2.80	3.41	3.84
11	2.17	2.08	2.06	2.27	2.89	3.50
12	1.76	1.67	1.65	1.84	2.45	3.19
13	1.43	1.34	1.32	1.49	2.07	2.90
14	1.15	1.08	1.06	1.21	1.76	2.65
15	0.93	0.86	0.84	0.98	1.49	2.41
16	0.75	0.69	0.68	0.80	1.26	2.20
17	0.61	0.56	0.54	0.65	1.07	2.00
18	0.49	0.45	0.43	0.52	0.90	1.82
19	0.40	0.36	0.35	0.43	0.77	1.66
20	0.33	0.29	0.29	0.36	0.67	1.52

Table 6.3. Maximum amount of crystallinity as a function of the minimum sequence length

Minimum sequence length	tacticity α					
ξ_{min}	0.50	0.55	0.60	0.70	0.80	0.90
1	100.00	100.00	100.00	100.00	100.00	100.00
2	75.00	75.25	76.00	79.00	84.00	91.00
3	62.50	61.64	61.60	64.30	71.20	82.90
4	50.00	49.14	49.20	52.12	60.32	75.59
5	40.62	40.51	39.33	42.27	51.10	68.87
6	32.81	31.68	31.46	34.28	43.30	62.74
7	26.56	25.42	25.17	27.80	36.68	57.16
8	21.48	20.50	20.13	22.55	31.08	52.08
9	17.38	16.47	16.11	18.28	26.33	47.45
10	14.06	13.23	12.88	14.83	22.31	43.23
11	11.38	10.64	10.31	12.03	18.90	39.39
12	9.20	8.55	8.25	9.75	16.01	35.89
13	7.45	6.88	6.60	7.91	13.56	32.70
14	6.02	5.54	5.28	6.41	11.49	29.80
15	4.87	4.47	4.22	5.20	9.74	27.15
16	3.94	3.60	3.38	4.22	8.25	24.74
17	3.19	2.91	2.70	3.42	6.99	22.54
18	2.58	2.35	2.16	2.77	5.92	20.54
19	2.08	1.91	1.73	2.25	5.02	18.72
20	1.66	1.57	1.39	1.84	4.27	17.07

This causes the melting point of these crystallites to be lower than that of pure syndiotactic crystallites. The orthorhombic crystallinity is formed more readily in syndiotactic materials: both the quantity (percentage of crystallinity) and the quality (melting point) are higher for syndiotactic or partly syndiotactic PVC.

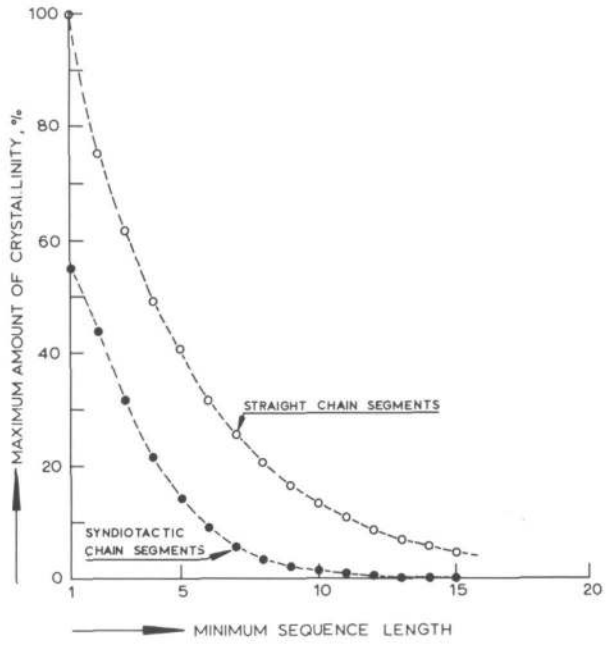

Figure 6.7. Maximum amount of crystallinity for an atactic PVC with $\alpha = 0.55$ as a function of minimum sequence length.

6.4.3. Nematic structures

The description of the nematic structure remains vague because there is so little information from the diffuse X-ray diffraction pattern. The distance between the chains in this kind of structure is only slightly larger than that in the orthorhombic lattice (5.4. and 5.3. A, respectively[92]). It is probable that the discontinuities which were described in the previous section can be accomodated in this kind of

structure. Figure 6.8. shows the cross-section of a PVC chain with such a chain defect. If neighbouring, aligned chains would contain similar discontinuities it is possible that these chains fit together. However, there is no evidence for this supposition and further experimental and theoretical research should be undertaken to elucidate the packing of the chains in the nematic state.

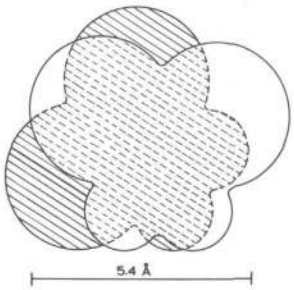

Figure 6.8. Cross-section of a PVC chain containing a discontinuity.

6.5. The amorphous phase

Earlier in this thesis (section 5.3.3.) the bulk polymer was described as consisting of straight chains in a more or less dense packing. This description explains that the difference in the densities of the crystalline and amorphous phases is small because the chains in the amorphous phase also have the extended conformation. However, the mechanical behaviour of the polymer cannot be explained by this model: a material consisting of nothing but straight chains would be very hard and brittle. Since this is not found there must be defects in the chains -comparable with dislocations in crystals- which give the chains their mobility.

When discussing the chain conformations in this thesis, a deliberate choice was made to construct only with trans pairs, which yield straight chains that could cause the crystallinity of PVC. With these pair conformations a large number of other chain conformations can be written

down. Some of these conformations give almost straight chains with occasional defects. These defects -called kinks- consist of a small parallel shift of straight chain segments which develop by a rotation around one or two monomer units. A molecular model of polyethylene on the basis of straight chains and kinks was published in many papers by Pechhold *et al.*[95-101]. This kink theory can also be applied to PVC: various kink conformations and the mobility of kinks in the chain were described in a recent paper[2]. According to this theory the amorphous phase in PVC consists of chains mainly in the extended conformation which do contain defects like discontinuities and kinks.

6.6. Primary and secondary crystallinity in PVC

The crystalline structures in PVC can now be interpreted. The primary crystallinity has the orthorhombic structure. The strongest evidence for this was given by Kockott[31] who showed that the X-ray reflections of atactic PVC disappear upon melting at 150°C. This melting point, which was also found in the calorimetric experimental work described in chapter 3, is lower than that of partly syndiotactic PVC. The introduction of atactic chain segments in the crystal lattice depresses the melting temperature. In copolymers of vinyl chloride and vinyl acetate the primary crystallinity is absent because the presence of the large acetate group in the chain prevents the crystallization in the orthorhombic lattice.

The formation of primary crystallinity requires the chains to be mobile which is achieved by dissolving the polymer in a good solvent. However, even then the crystallization appears to be very difficult since it only occurs when the precipitation is performed very slowly. Therefore it is not surprising that recrystallization of the orthorhombic crystals does not occur in the bulk of the polymer where the mobility of the chains is very much more restricted.

Upon annealing secondary crystallinity is formed. Presumably, this type of crystallinity has a nematic structure although Lebedev[30] also found orthorhombic X-ray reflections after annealing PVC at 110°C. The

packing of the chains is less ideal compared with that in the orthorhombic lattice. This results in a lower melting temperature and a lower heat of fusion. In copolymers of vinyl chloride with vinyl acetate secondary crystallinity is also formed which demonstrates that a strict chain regularity is not necessary.

Secondary crystallinity is not formed unless the primary crystallites have been melted by prior heating. The binding of the chains in the orthorhombic crystals prevents the alignment of the chains outside these crystallites. Once the primary crystallites have been melted the mobility of the chains in the bulk is large enough for the formation of nematic structures.

6.7. Conclusions

1. Isotactic straight chain segments contribute to the formation of orthorhombic crystallinity and nematic structures.
2. The value found by calculating the amount of crystallinity originating from atactic chain segments is in agreement with experimental data.
3. The primary crystallinity in PVC has an orthorhombic structure.
4. The secondary crystallinity in PVC presumably has a nematic structure.

LIST OF SYMBOLS

a	constant in equation 5.4	A^{-1}
a, b, c	orthorhombic axes	
d	distance between bonded atoms	A
E	energy	kcal/mole
E	modulus of elasticity	kgf/cm^2
F^N_{syndio}	fraction of polymer present as syndiotactic chain segments of N sequences	
$F^N_{straight}$	fraction of polymer present as straight chain segments of N sequences	
G_ℓ	conformation parameter (gauche-left)	
G_r	conformation parameter (gauche-right)	
ΔH	heat of fusion	cal/mole
i	isotactic sequence	
k	reaction rate constant	
K	constant in equation 5.4	kcal/mole
K'	constant in equation 5.4	$kcal \cdot A^6/mole$
(L)	left-handed monomer unit	
N	number of monomer sequences, length of chain segment	
p	probability	
q	charge (equations 5.2 and 5.3)	e.s.u.
	dimension of q^2:	kcal·A/mole
r	distance between nonbonded atoms	A
R	gas constant	$kcal/mole \cdot {}^oK$
(R)	right-handed monomer unit	
s	syndiotactic sequence	
S_{XY}	nomenclature of conformation in IR analysis	
T	temperature	^oK
T	conformation parameter (trans)	

α	tacticity	
μ	dipole moment	Debije
ξ_{min}	minimum sequence length	
ρ	density	g/cm^3
τ	chemical shift (NMR analysis)	

REFERENCES

1. International Union of Pure and Applied Chemistry, Information Bulletin 35, XXVth Conference, Cortina Italy, june 1969, 39,40.
2. J.H. Gisolf, J.A. Juijn, Kolloid - Z.Z. Polym. 239, 545 (1970).
3. Y. Abe, M. Tasumi, T. Shimanouchi, S. Satoh, R. Chûjô, J. Polym. Sci. Part A-1, 4 1413 (1966).
4. F.A. Bovey, Polym. Eng. Sci. 7, 128 (1967).
5. F.A. Bovey, E.W. Anderson, D.C. Douglas, J. Chem. Phys. 39, 1199(1963).
6. D. Doskocilová, J. Štokr, B. Schneider, M. Pivcová, M. Kolínsky, J. Petránek, D. Lím, J. Polym. Sci. Part C, 16, 215 (1967).
7. P.E. McMahon, W.C. Tincher, J. Mol. Spectrosc. 15, 180 (1965).
8. K.C. Ramey, J. Chem. Phys. 70, 2525 (1966).
9. L. Cavalli, G.C. Borsini, G. Carraro, G. Confalonieri, J. Polym. Sci. Part A-1, 8, 801 (1970).
10. U. Johnsen, J. Polym. Sci. 54, S6 (1961).
11. T. Yoshino, J. Komyama, J. Polym. Sci. Part B, 3, 311 (1965).
12. F.A. Bovey, F.P. Hood, E.W. Anderson, R.L. Kornegay, J. Phys. Chem. 71, 312 (1967).
13. J. Bargon, K.-H.Hellwege, U. Johnsen, Makromol. Chem. 95, 187 (1966).
14. E. Enomoto, M. Asahina, S. Satoh, J. Polym. Sci. Part A-1, 4, 1373 (1963).
15. S. Satoh, J. Polym. Sci. Part A, 2, 5221 (1964).
16. W.C. Tincher, Makromol. Chem. 85, 20 (1965).
17. G. Talamini, G. Vidotto, Makromol. Chem. 100, 48 (1967).
18. H. Germar, K.-H.Hellwege, U. Johnsen, Makromol. Chem. 60, 106 (1963).
19. H. Germar, Kolloid - Z.Z. Polym. 193, 25 (1963).
20. J. Stokr, B. Schneider, M. Kolínsky, M. Ryska, D. Lím, J. Polym. Sci. Part A-1, 5, 2013 (1967).
21. H.U. Pohl, D.O. Hummel, Makromol. Chem. 113, 190 (1968).
22. H.U. Pohl, D.O. Hummel, Makromol. Chem. 113, 203 (1968).
23. J.W.L. Fordham, P.H. Burleigh, C.L. Sturm, J. Polym. Sci. 41, 73 (1959).

24. J.W.L. Fordham, J. Polym. Sci. 39, 321 (1959).
25. P.J. Flory, Trans. Faraday Soc. 51, 848 (1955).
26. K.-H. Hellwege, U. Johnsen, D. Kockott, Kolloid - Z.Z. Polym. 194, 5 (1964).
27. K.-H. Illers, Makromol. Chem. 127, 1 (1969).
28. A. Konishi, K. Nambu, J. Polym. Sci. 54, 209 (1961).
29. G. Natta, P. Corradini, J. Polym. Sci. 20, 262 (1956).
30. V.P. Lebedev, N.A. Okladnov, K.S. Minsker, B.P. Shtarkman, Vysokomol. soedin 7, 655 (1965) (translated in Polym. Sci. USSR 7, 724 (1965)).
31. D. Kockott, Kolloid - Z.Z. Polym. 198, 17 (1964).
32. A.T. Walter, J. Polym. Sci. 13, 207 (1954).
33. F.P. Reding, E.R. Walter, F.J. Welch, J. Polym. Sci. 56, 225 (1962).
34. C.E. Anagnastopoulos, A.Y. Coran, H.R. Gamrath, J. Polym. Sci. 4, 181 (1960).
35. A. Nakajima, H. Hamada, S. Hayashi, Makromol. Chem. 95, 40 (1966).
36. J.E. Clark, Polym. Eng. Sci. 7, 137 (1967).
37. V.P. Lebedev, N.A. Okladnov, M.N. Shlykova, Plast. Massy, april 1968, 8 (translated in Sov. Plast., april 1968, 10).
38. A. Michel, Rev. Gen. Caout. Plast. 46, 227, 365 (1969).
39. J.A. Juijn, J.H. Gisolf, W.A. de Jong, Kolloid - Z.Z. Polym. 235, 1157 (1969).
40. H. Wilski, Kolloid - Z.Z. Polym. 210, 37 (1966).
41. Th. Grewer, H. Wilski, Kolloid - Z.Z. Polym. 226, 46 (1968).
42. H. Wilski, Kolloid - Z.Z. Polym. 238, 426 (1970).
43. P.V. McKinney, C.R. Foltz, J. Appl. Polym. Sci. 11, 1189 (1967).
44. Yu.A. Sharonov, M.V. Volkenshtein, Vysokomol. soedin 4, 917 (1962).
45. Yu.A. Sharonov, M.V. Volkenshtein, Fiz. Tverd. Tela 5, 590 (1963) (translated in Sov. Phys. Solid State 5, 429 (1963)).
46. A.J. Kovacs, Fortschr. Hochpolym. Forsch. 3, 394 (1963).
47. J.M. O'Reilly, F.E. Karasz, J. Polym. Sci. Part C, 14, 49 (1966).
48. K. Ueberreiter, W. Bruns, Ber. Bunsenges. Phys. Chem. 70, 17 (1966).
49. K. Ueberreiter, Kolloid - Z.Z. Polym. 216/217, 217 (1967).

50. R.D. Heap, R.H. Norman, RAPRA research report 149 (1966).
51. G. Pezzin, N. Gligo, J. Appl. Polym. Sci. 10, 1 (1966).
52. P. Kratochvíl, V. Petrus, P. Munk, M. Bohdanecký, K. Solc, J. Polym. Sci. Part C, 16, 1257 (1967).
53. A.T. Walter, J. Polym. Sci. 13, 207 (1954).
54. I. Tomaszewska, J. Raczynska, Z. Roszkowski, Plaste Kaut. 15, 353 (1968).
55. J.H. Gisolf, Plastica 19, 430 (1966).
56. G.A. Razuvayev, G.G. Petakhov, V.A. Dodonov, Vysokomol. soedin. 3, 1549 (1961) (translated in Polym. Sci. USSR, 3, 1020 (1962)).
57. J.D. Cotman, Ann. N.Y. Acad. Sci. 57, 417 (1953).
58. G. Bier, H. Kramer, Kunststoffe 46, 498 (1956).
59. G.M. Burnett, F.L. Ross, J.N. Hay, J. Polym. Sci. Part A-1, 5, 1467 (1967).
60. G. Boccato, A. Rigo, G. Talamini, F. Zilio - Grandi, Makromol. Chem. 108, 218 (1967).
61. C.S. Marvel, J.H. Sample, M.F. Roy, J. Amer. Chem. Soc. 61, 3241 (1939).
62. H.E. Fierz-David, H. Zollinger, Helv. Chim. Acta 28, 455 (1945).
63. Tables of Interatomic Distances and Configuration in Molecules and Ions, Special Publication 18 (supplement), The Chemical Society, London, 1965, S 14s, S 17s and S 18s.
64. R.E. Robertson, J. Phys. Chem. 69, 1575 (1965).
65. Yu.V. Glazkovskii, Yu.G.Papulov, Vysokomol. soedin. ser. A, 10, 492 (1968) (translated in Polym. Sci. USSR 10, 569 (1968)).
66. T.L. Hill, J. Chem. Phys. 16, 399, 938 (1948).
67. A.D. Crowell, J. Chem. Phys. 29, 446 (1958).
68. E.A. Mason, M.M. Kreevoy, J. Amer. Chem. Soc. 77, 5808 (1955).
69. M.M. Kreevoy, E.A. Mason, J. Amer. Chem. Soc. 79, 4851 (1957).
70. M.V. Volkenshtein, Configurational Statistics of Polymer Chains, J. Wiley, London, 1963, 60.
71. T.M. Birshtein, O.B. Ptitsyn, Conformation of Macromolecules, J. Wiley, London, 1966, 31.

72. K.S. Pitzer, Discuss. Faraday Soc. 10, 66 (1951).
73. S. Krimm, Pure Appl. Chem. 16, 369 (1968).
74. S. Krimm, S. Enomoto, J. Polym. Sci. Part A, 2, 669 (1964).
75. S. Mizushima, T. Shimanouchi, K. Nakamura, M. Hayashi, S. Tsuchiya, J. Chem. Phys. 26, 970 (1957).
76. C.G. Opaskar, Ph.D. Thesis, Univ. of Michigan, 1966.
77. T. Shimanouchi, M. Tasumi, Spectrochim. Acta 17, 755 (1961).
78. S. Krimm, V.L. Folt, J.J. Shipman, A.R. Berens, J. Polym. Sci. Part B, 2, 1009 (1964).
79. S. Krimm, A.R. Berens, V.L. Folt, J.J. Shipman, Chem. Ind. (London) 1512 (1958).
80. S. Krimm, Fortschr. Hochpolym. Forsch. 2, 51 (1960).
81. T. Shimanouchi, S. Tsuchiya, S. Mizushima, J. Chem. Phys. 30, 1365 (1959).
82. M. Takeda, K. Iimura, J. Polym. Sci. 57, 383 (1962).
83. K. Iimura, M. Takeda, J. Polym. Sci. 51, S51 (1961).
84. Yu.V. Glaszkovskii, V.E. Zgayevskii, S.P. Ruchinskii, N.M. Bakardzhiyev, Vysokomol. soedin 8, 1472 (1966) (translated in Polym. Sci. USSR 8, 1622 (1966)).
85. S. Krimm, J.J. Shipman, V.L. Folt, A.R. Berens, J. Polym. Sci. Part B, 3, 275 (1965).
86. J.L. Koenig, D. Druesedow, J. Polym. Sci. Part A-2, 7, 1075 (1969).
87. D.M. White, J. Amer. Chem. Soc. 82, 5678 (1960).
88. A.R. Berens, V.L. Folt, Trans. Soc. Rheol. 11, 95 (1967).
89. L.I. Vidyaikina, N.A. Okladnov, B.P. Shtarkman, Vysokomol. soedin 8, 390 (1966) (translated in Polym. Sci. USSR 8, 425 (1966)).
90. R.W. Smith, C.E. Wilkes, J. Polym. Sci. Part B, 5, 433 (1967).
91. A. Nakajima, S. Hayashi, Kolloid - Z.Z. Polym. 229, 12 (1969).
92. M. Mammi, V. Nardi, Nature (London), july 1963, 247.
93. V. Nardi, Nature (London), august 1961, 563.
94. V.P. Lebedev, N.A. Okladnov, M.N. Shlykova, Vysokomol. soedin ser. A, 9, 495 (1967) (translated in Polym. Sci. USSR 9, 553 (1967)).
95. W. Pechhold, Kolloid - Z.Z. Polym. 228, 1 (1968).

96. W. Pechhold, S. Blasenbrey, S. Woerner, Kolloid - Z.Z. Polym. 189, 14 (1963).
97. W. Pechhold, S. Blasenbrey, Kolloid - Z.Z. Polym. 216/217, 235 (1964).
98. S. Blasenbrey, W. Pechhold, Ber. Bunsenges. Phys. Chem. 74, 784 (1970).
99. W. Pechhold, S. Blasenbrey, Kolloid - Z.Z. Polym. 241, 955 (1970).
100. P.C. Hägele, W. Pechhold, Kolloid - Z.Z. Polym. 241, 977 (1970).
101. G. Wobser, S. Blasenbrey, Kolloid - Z.Z. Polym. 241, 985 (1970).

SUMMARY

This thesis deals with crystalline phenomena in polyvinyl chloride. Melting effects in both rigid and plasticized PVC were studied experimentally by differential scanning calorimetry. Theoretical investigations on the structure of the chain and molecular packing in crystallites were performed in order to explain the occurrence of crystallinity in atactic PVC.

The monomer unit in the PVC chain has two stereoisomeric configurations and as a consequence isotactic as well as syndiotactic sequences occur. The tacticity of the material is a function of polymerization temperature: as the reaction temperature is lower an increasingly syndiotactic polymer is obtained. The relation between tacticity and polymerization temperature is described theoretically in accordance with literature data on measurements of the tacticity by nuclear magnetic resonance and infrared spectroscopy.

The syndiotactic polymerizates are more crystalline than the commercial atactic PVC grades. Therefore, it is usually assumed that only the syndiotactic part of the PVC is crystallizable. However, Flory's theory on partly crystallizable copolymers predicts a crystalline content which is considerably lower than the values found experimentally. As a consequence, it is concluded that isotactic chain segments crystallize along with syndiotactic parts.

The melting phenomena in commercial atactic PVC have been studied experimentally. Measurements with a Differential Scanning Calorimeter show an endothermic melting effect in thermally untreated PVC which commences at about 150°C and extends into the decomposition range. The primary crystallinity which is responsible for this effect is higher in syndiotactic PVC and lower or absent in copolymers of vinyl chloride and vinyl acetate, as compared with commercially produced PVC. The measured melting temperature (150 - > 200°C) and the calculated heat of fusion (850 cal/mole) agree with literature data.

A second melting effect is found after annealing the polymer for some time at a temperature above the glass transition region. This secondary crystallinity is much less dependent on chain regularity. It melts at a lower temperature (100 - 160°C) and has a lower heat of fusion (400 cal/mole).

The formation of secondary crystallinity has an important consequence for the properties of plasticized PVC. In this material crystallites are formed during storage at room temperature which can be detected calorimetrically. As a result, the density and stiffness of the material increase. Similar behaviour is shown by related materials such as copolymers of vinyl chloride with vinyl acetate and highly chlorinated polyethylene.

The theoretical part of this thesis starts with an analysis of the chain structure in which the influence of configuration and conformation is investigated. The study of the conformations of monomer units and monomer pairs leads to the conclusion that three different regular chain structures exist: the syndiotactic straight zig-zag chain, the isotactic helix and an isotactic straight chain. It appears that the syndiotactic straight chain has an isotactic counter part which clearly differs from the isotactic helix conformation. The energies of the three chains are calculated from steric potentials and dipole interactions. The results show that the energy of the isotactic straight chain is only slightly higher than that of the helix.

The chain structure can be studied experimentally by nuclear magnetic resonance and infrared spectroscopy. Literature data on infrared measurements strongly support the postulate that isotactic straight chains contribute to the crystallinity of PVC.

The crystalline packing is described extensively in the literature. Electron microscopy of single crystals and X-ray measurements show that PVC crystallizes in an orthorhombic lattice. However, in bulk PVC also less ideal, nematic, structures are found.

The present work reveals that the isotactic straight chain fits into the orthorhombic lattice. With the aid of atomic models it is shown

that even atactic chain segments can crystallize in an orthorhombic lattice. A calculation of the length of straight atactic chain segments is presented and when the results are introduced into Flory's theory satisfactory agreement between the observed and theoretically predicted amount of crystallinity of about 10% is obtained. The crystallization in nematic structures does not require a strict regularity of the chains and, therefore, a higher fraction of the polymer is able to crystallize in this manner.

Finally, it is concluded that the primary crystallinity in PVC has an orthorhombic structure. The secondary crystallinity most probably has a nematic structure.

SAMENVATTING

Kristallijne verschijnselen in polyvinylchloride worden in dit proefschrift beschreven. Het experimenteel gedeelte bestaat voornamelijk uit calorimetrisch onderzoek naar smeltverschijnselen in weekgemaakt zowel als niet-weekgemaakt PVC. In het theoretische gedeelte worden de ketenstructuur en de kristallijne structuur bestudeerd teneinde de aanwezigheid van kristalliniteit in atactisch PVC te verklaren.

De monomere eenheid in de PVC-keten heeft twee stereoisomere configuraties en als gevolg daarvan komen zowel isotactische als syndiotactische sekwenties voor. De tacticiteit blijkt een functie van de polymerisatietemperatuur te zijn: bij lagere temperatuur wordt een meer syndiotactisch polymeer gevormd. Dit verband tussen tacticiteit en polymerisatietemperatuur wordt theoretisch beschreven, in overeenstemming met gegevens uit de literatuur betreffende metingen van de tacticiteit met behulp van kernspinresonantie en infraroodspectroscopie.

De syndiotactische polymerisaten zijn kristallijner dan de commerciële, atactische PVC's. Hierdoor ontstond de voor de hand liggende gedachte dat alleen het syndiotactische deel van het PVC kristalliseerbaar is. Een berekening volgens de theorie van Flory leert echter dat de kristalliniteit in werkelijkheid veel hoger is dan volgens deze aanname kan worden verklaard. Daarom wordt geconcludeerd dat naast het syndiotactische deel ook de isotactische ketens moeten bijdragen tot de vorming van kristalliniteit.

De smeltverschijnselen in atactisch PVC werden experimenteel bestudeerd. De metingen met behulp van "Differential Scanning Calorimetry" tonen aan dat er in PVC zonder thermische voorbehandeling een smelteffect aanwezig is dat begint bij ongeveer 150°C en dat doorloopt tot in het ontledingsgebied. De op deze manier waargenomen primaire kristalliniteit is, in vergelijking met die in atactisch PVC, hoger in syndiotactisch PVC en lager of afwezig in copolymeren van vinylchloride en